Metasomatic processes and environment.

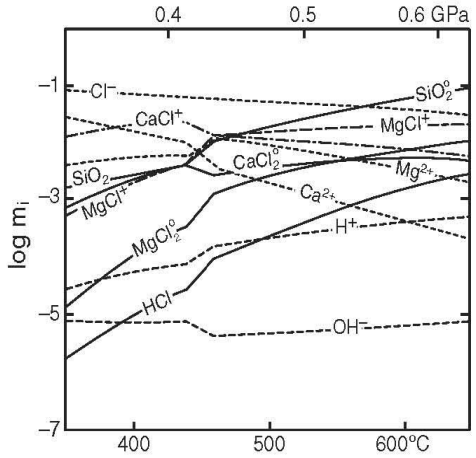

FIGURE 4 Speciation in aqueous–chloride fluids calculated for an ultramafic bulk composition, assuming a geothermal gradient of 0.1°C/bar. m_i is the molality of species i in the fluid. Solid curves represent neutral associated species. After Eugster and Baumgartner (1987). Copyright © The Mineralogical Society of America.

(dashed curves for Cl^-, Mg^{2+}, Ca^{2+}, etc.) tend to decrease with increasing grade (H^+ is a notable exception), whereas associated ions ($MgCl^+$ and $CaCl^+$) and uncharged species (SiO_2°, $CaCl_2^\circ$ and $MgCl_2^\circ$) all increase. Na and K, although usually quite soluble, are not considered in Figure 4 because of their low abundance in ultramafic systems. Similarly, Fe is not considered in Figure 4, although Eugster and Gunter (1981) found that Fe is generally more soluble than Mg.

Walther and Helgeson (1980) found that Ca^{2+} is a thousand times more soluble than Mg^{2+} in metamorphic CO_2-H_2O fluids associated with calcite-bearing calcareous rocks, whereas Mg^{2+} may be more soluble in carbonated metamorphosed ultramafics (which is apparent at high temperatures in Figure 4). Helgeson et al. (1981), in their weighty monograph, summarized aqueous solutions as ranging from nearly pure H_2O-CO_2 fluids to concentrated ore-forming solutions, composed predominantly of NaCl, KCl, $CaCl_2$, and $MgCl_2$, with lesser concentrations of bicarbonates and sulfates–bisulfates, together with minor H_2S, SiO_2, and chlorides of Al, Fe, Zn, Pb, Cu, Ag, etc.

Characterization of metamorphic fluids is still in the early stages of development, and the speciation obviously varies, but we are now aware that metamorphic fluids may contain a host of volatile and dissolved species. Dissolved constituents are present mostly in low concentrations, and the relative abundances are commonly Na and K > Si, Ca, Fe, and Mg > Al. In addition to Al, the high field strength (HFS) minor and trace elements such as Ti, Cr, Zr, Y, and Ni are generally insoluble in aqueous fluids, hence their use as indicators of the paleo-tectonic environment of metamorphosed igneous rocks in discrimination diagrams. The high solubility of large-ion lithophile elements (i.e., Rb, Cs, Ba, Pb, Sr, U) explains the "decoupling" of soluble LIL and insoluble HFS elements due to the interaction of hydrous fluids with the mantle source of subduction-related magmas.

1.2 The Role of Fluids in Metamorphism

We are becoming increasingly aware that fluids are a critical participant in metamorphic and igneous processes. Aqueous fluids reduce the melting point of rocks and enhance melting. They are also released by rising and cooling magmas where they generate pegmatites and ores. Mixtures of exhaled and meteoric fluids feed hydrothermal systems above plutons and in shallow permeable areas of regional metamorphism. As discussed above, fluids released over time by devolatilization reactions may be equivalent to over 10% of the volume of a rock. Fluids can dissolve material, transport heat and solutes, precipitate minerals, exchange components as they react with minerals, and catalyze deformation processes by weakening rocks. Contact metamorphic aureoles are largest where fluids are available to transport heat and matter. Fluid buffering versus open-system behavior may control the progress of metamorphism and mineral reactions in many situations. Release and flow of fluids absorb and transfer large quantities of heat and matter. The absorption and transfer by fluids of heat alone may have profound effects upon the temperature distribution in a contact aureole or even throughout an orogenic belt, and hence upon the geologic evolution of an area (Bickle and MacKenzie, 1987). Metamorphism is thus far more complex than simple reequilibration of minerals to increased temperature and/or pressure upon burial or proximity to an intrusion, as it is commonly perceived.

Fluid transport through rocks has a profound effect on the processes mentioned in the preceding paragraph. Although flow through a porous medium is certainly the most efficient mechanism for fluid transport, rocks are highly porous only in the shallow crust. Below 10 km, a continuous network of large open pore spaces is closed by compaction and recrystallization. Motion of a fluid along fractures or of an intergranular fluid along grain boundaries are the only ways that fluids can migrate in the deeper crust. We will return to this concept in more detail shortly.

2 METASOMATISM

Metasomatism is defined as metamorphism accompanied by changes in whole-rock composition. Because volatiles are so readily released and mobilized during metamorphism, changes in the volatile content of rocks are generally excluded, and the chemical changes that constitute metasomatism (*sensu-stricto*) are usually restricted to the redistribution of nonvolatile species. You may be familiar with the changes in mineralogy in the contact aureole at Crestmore, California, and found that the mineral assemblages were readily explained by a progressive increase in the amount of SiO_2 in the country rock marbles as the igneous contact was

approached. SiO_2 was presumably derived from the quartz monzonite porphyry and transported as dissolved silica in aqueous fluids circulating away from the body. Other examples of metasomatism discussed previously include Na metasomatism associated with ocean floor metamorphism, alkali metasomatism associated with carbonatites that produce fenites, mantle metasomatism, infiltration, and depletion of granulites.

Metasomatism is most dramatically developed in situations where rocks of highly contrasting composition are juxtaposed and elements move easily. Common examples include:

Shallow plutons, particularly where siliceous magmas contact calcareous or ultramafic rocks and fluids are circulated through open fractures.

Layers, lenses, and pods with contrasting composition in rocks undergoing metamorphism: ultramafic pods in pelites or carbonates, interbedded carbonate and pelitic sediments.

Veins where fluids equilibrate with one rock type and then migrate into a contrasting rock type along a fracture.

For a detailed review of the types of metasomatism and their general characteristics, see Barton et al. (1991a). Their main categories are (1) alkaline and alkali earth metasomatism, (2) hydrolytic alteration (hydrogen metasomatism), (3) volatile additions, (4) fenitization, (5) carbonate-hosted skarn formation, and (6) alteration of ultramafics.

2.1 Metasomatic Processes

The Russians have an extensive literature on metasomatism, largely because of the pioneering work of D. S. Korzhinskii (1959 and 1970 translations in English). Korzhinskii first distinguished the two principal processes of mass transfer in rocks: diffusion and infiltration. Although conceptually distinguishable, these two processes are probably end-members of a continuous spectrum of combined mechanisms.

2.1.1 DIFFUSION **Diffusion** is the process by which components move *through* another medium, either a solid (lattice diffusion) or a stationary fluid. Diffusion is driven by chemical potential (μ) gradients. If the chemical potential of a species is higher in one area than in another, migration of that species from the area of higher μ to that of lower μ will lower the free energy of the whole system. Matter will thus tend to migrate down chemical potential gradients if there is nothing to inhibit such migration. **Bimetasomatism** refers to the diffusion of components in opposite directions in a reciprocal or exchange fashion. The migration of MgO in one direction and SiO_2 in the opposite direction in the hypothetical column of J. B. Thompson (1959), discussed below, is an example of bimetasomatism.

At a first approximation, diffusion is described by **Fick's first law**, proposed by A. Fick in 1855:

$$J_x(g\,\mathrm{cm}^{-2}\,s^{-1}) = -D(\mathrm{cm}^{-2}\,s^{-1})\frac{dC\,(g\,\mathrm{cm}^{-3})}{dx\,(\mathrm{cm})} \qquad (6)$$

which states that the flux (J_x) of material in one direction (x) is proportional to the concentration gradient $(-dC/dx)$. We now recognize that the chemical potential gradient is more appropriate than concentration. The proportionality constant (D) is called the **diffusion coefficient**. Diffusion coefficients for various materials are determined empirically and increase with temperature (log D decreases almost linearly with $1/T$ in kelvin). As a result, the material flux increases with both temperature and the steepness of the concentration gradient. Diffusion coefficients are very small for most silicate minerals. Typical D values are on the order of 10^{-15} cm^2/sec or less at 1000°C. We can estimate the effectiveness of diffusion from the approximation (Kretz, 1994, p. 283):

$$\overline{x} \approx (Dt)^{1/2} \qquad (7)$$

where $\overline{x}$ is the mean displacement of material in time t (in seconds). From this equation we can calculate that, if $D = 10^{-15}$, a component will diffuse about 1 cm through a mineral in about 100 million years under typical metamorphic temperatures. This is dreadfully slow and suggests that diffusion of material through minerals is an ineffective metasomatic process. The preservation of fine compositional zoning in plagioclase and garnet, and of coronites and reaction rims in high-grade (dry) metamorphic rocks, supports this conclusion. Of course, geothermobarometry relies upon the sluggishness of diffusive re-equilibration upon cooling.

Diffusion is much more effective through a fluid phase, in which diffusion coefficients are on the order of 10^{-4} or greater. This would allow mean displacements on the order of a few meters per year. If diffusion is to occur over such distances a fluid must be present, of course, and it must be sufficiently interconnected as a grain boundary network. Whether it is interconnected or not depends upon the quantity of fluid present and the dihedral angle (θ) of fluid–mineral triple points. Even in rocks of very low porosity, an intergranular fluid can form a continuous grain boundary network if the dihedral angle is sufficiently low. For the fluid to form a surface film that wets the surfaces of the grains requires a dihedral angle of only a few degrees. Such a film is unnecessary, however, for an interconnected fluid network. It is sufficient only that the fluid forms a network of interconnected tubes at grain edges (Figure 5a and c). For fluids occupying only 1 to 2% of a rock volume, this is possible when the dihedral angle of the fluid is less than 60°. When θ is greater than 60°, the tubes pinch off and the fluid beads up as isolated pockets at grain–edge intersections (Figure 5b).

Brenan (1991) summarized most of the experimental data on dihedral angles of fluids in mineral aggregates. Experiments with quartz in H_2O-CO_2 mixtures yield dihedral angles that increase from 55° in pure H_2O to over 90° if $X_{CO_2} > 0.86$. Addition of about 10% NaCl, KCl, or CaF_2

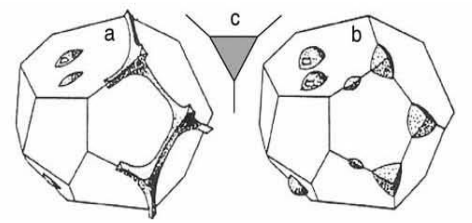

FIGURE 5 Three-dimensional distribution of fluid about a single grain at $\theta < 60°$ (left) and $\theta > 60°$ (right). In the center is a cross section through a fluid tube at the intersection of three mineral grains for which $\theta = 60°$. After Brenan (1991). Copyright © the Mineralogical Society of America.

reduced θ by 10 to 15°. Decreasing pressure from 1.0 → 0.6 GPa also tends to raise θ by 10 to 20°. Initial data from natural rocks seem to agree with the experimental findings that θ is generally >60°, indicating that a continuous grain-surface film is rare, and that an interconnected tube-like network of fluid is unlikely at middle to upper crustal levels, unless the fluids are very saline and H_2O-rich. Although fluids can allow much more rapid diffusion, it appears that fluids, at least under hydrostatic conditions in which volatiles are not being released by reactions, usually exist as isolated pockets. Diffusion through fluid pockets and along dry grain boundaries, however, is still much more rapid than through a crystal lattice.

2.1.2 INFILTRATION **Infiltration** refers to passive mass transfer of solute species carried in a moving fluid medium. Whereas diffusion occurs in response to internal chemical potential gradients, infiltration is driven by external fluid pressure gradients that cause the fluids to move. Pervasive fluid flow through a porous-permeable medium is described by **Darcy's law**. The Darcy flux increases with increased permeability, fluid pressure gradients, and reduced fluid viscosity. Darcy's law is more complex than we need deal with here. If you are interested, see equation 1 in Ague (2003) and the ensuing discussion. Fluids in motion permit much more extensive transport of matter than does diffusion. Regional-scale mass transport is not possible via diffusion alone and can only occur with the aid of infiltrating fluids. Evidence for fluid flow is widespread, including the progressive devolatilization of rocks with increasing metamorphic grade, the existence of geothermal springs and fluids encountered in deep wells, nearly ubiquitous veins filled with deposited minerals, hydrous alteration along shear zones and thrusts, metasomatic replacement textures, and variations in stable isotopes that are best explained by exchange between host rocks and introduced fluids.

One must wonder how such pervasive fluid flow is possible in light of the evidence that an interconnected network of fluid channels is not stable with typical rock porosities under hydrostatic conditions. Permeability may be enhanced, however, in several possible ways (see the reviews by Walther, 1990; Brenan, 1991; Ferry, 1991, 1994; Rumble, 1994; and Ague, 2003). Among the more popular ideas that have been proposed are the following.

Microfractures in crystalline rocks were first recognized by Adams and Williamson (1923). Microfractures are believed to be disc-shaped slits and are known to affect field-measured bulk transport properties, such as electrical resistivity and permeability, and must therefore form an interconnected network (Ferry, 1994). How pervasive these small cracks are in nature is not yet known. Many microfractures are now healed (recognizable as planar arrays of trapped fluid inclusions), suggesting that they may be transient.

During devolatilization reactions the fluid pressure increases to the point that it becomes greater than the tensile strength of the rocks, resulting in fractures. The process is called **hydraulic fracturing**. Fluids, being less dense than rocks, may move in these fractures as a result of their own buoyancy, promoting upwardly directed fluid-filled hydrofractures. This buoyancy mechanism may be responsible for significant upward metamorphic fluid flow. John Walther developed a model by which devolatilization reactions and expansion of pore fluids during active metamorphism resulted in fluid flow toward the surface along fracture networks (Walther and Orville, 1982; Walther and Wood, 1984; Wood and Walther, 1986; Walther, 1990). Calculations suggest that an isolated fluid-filled fracture can propagate upward at rates approaching 1 km/hr (Rumble, 1994). This rapid propagation of fluid-filled cracks can result in significant fluid fluxes. To the extent that devolatilization reactions are active during discrete intervals of prograde metamorphism (at discontinuous isograds), and because fracture propagation eventually dissipates the fluid pressure, this type of enhanced permeability may be largely episodic. To the extent that such reactions are continuous or buffered, fluids may also be released in lesser quantities on a more prolonged basis.

Many devolatilization reactions produce a smaller volume of solid products than was occupied by the mineral reactants. The volume reduction has been called **reaction-enhanced permeability** (Rumble, 1994). Marchildon and Dipple (1998) and Dipple and Gerdes (1998) discussed the positive feedback in which fluid flow (e.g., flow in a contact aureole related to pluton emplacement) induces mineral reactions, which increase permeability, which in turn enhance fluid flow, etc. This process, which they called **flow focusing**, results in enhanced flow in some areas and irregularly shaped reaction zones. For the same reasons stated above, this type of enhanced permeability may be episodic below the shallowest depths. Russian researchers have also recognized a process known as **thermal decompaction**, which is the creation of voids in rocks upon heating due to the anisotropic expansion of the mineral grains and their variable orientations in rocks (see Zaraisky and Balashov, 1995).

If a rock is subjected to non-isostatic stress during metamorphism, permeability may be enhanced by **dilatancy pumping** (Sibson et al., 1975). Rocks dilate due to rapidly increasing numbers of microfractures just prior to failure under increasing stress. These fractures dilate and draw fluid into the stressed rock. Stress is released upon failure and the fractures collapse, expelling the fluid. The process can be repeated during applied stress, but is self-limiting because the fluid weakens the rock, and a rock with saturated pores will

dilate less before failure (Murrell, 1985). More elaborate models for fluid pumping have been proposed by Etheridge et al. (1984) and Oliver et al. (1990).

Although direct evidence for an interconnected network of cracks in rocks of moderate or greater depth is presently lacking, the models above suggest that relatively large fluid fluxes are at least possible. Contact metamorphism is particularly likely to have large, although local, fluid fluxes. Steep temperature and compositional gradients exist near the igneous contact. At low pressure, the porosity of the country rocks is likely to be high, and fracture systems associated with intrusion will usually be extensive, so that expelled magmatic fluids and available meteoric water will be convectively recirculated through the aureole. Flow, however, is probably localized along fractures and in permeable lithologies (see models and reviews by Norton and Knight, 1977; Barton et al., 1991b; Ferry, 1994; and Hanson, 1995).

Several investigators have attempted to estimate the quantity of fluid to pass through a given volume of rock over time, usually expressed as **time-integrated fluid:rock ratios**. Such ratios are not to be confused with porosity, which is the instantaneous ratio of fluid to rock. Connolly (1997) estimated porosity during metamorphism to be 0.1% to 0.001% of rock volume. Time-integrated fluid:rock ratios, however, are intended to reflect the extent of infiltration and flow over the duration of a metamorphic cycle. For example, Rumble et al. (1982) used the progress of the calcite + quartz → wollastonite + CO_2 reaction to estimate the quantity of fluid evolved during metamorphism of a bed containing silicified brachiopods at the Beaverbrook fossil locality in New Hampshire. The amount of wollastonite in some of the rocks was about 70%, far more than could be produced if the fluid were internally buffered. They calculated the amount of infiltrated fluid required to produce the "excess" wollastonite and derived a volume fluid:rock ratio of 4.6/1, so rocks containing 70% Wo had a volume of at least 4.6 times as much fluid pass through as there was rock. These estimates assume that the fluid is pure H_2O. If CO_2 were present, or if more fluid passed through without reaction, the fluid:rock ratios would have to be greater, so that all fluid:rock ratios are really *minimum* estimates. Wood and Walther (1986) cited estimates of fluid:rock ratios, based on reaction progress of isotopic exchange, ranging from 1 to 5, and calculated that the deposition of 1% quartz in metamorphosed pelites requires a fluid:rock ratio of 6/1.

Calculations of mass balance along a flow path, integrated over time, yield estimates of fluid flux as a volume of fluid passing through a specified rock area (the **time-integrated fluid flux**, or q_{TI}). Ague (2003) reviewed several mathematical approximations for q_{TI} (see Problem 1 for an example). Figure 6 summarizes several estimates of q_{TI} from Ague's (2003) review. Ague (1994a) estimated an average pervasive flow during regional metamorphism of $10^{2.7} \pm 0.5$ m^3 of fluid passed through each m^2 cross section of rock (shaded area in Figure 6). Methods of estimating such fluxes vary. For example, the work summarized by Ferry (1994) is based on mass balance using stable isotope

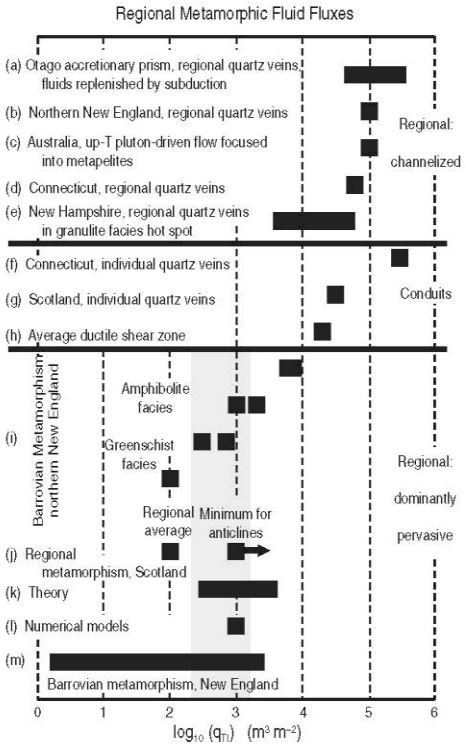

FIGURE 6 Selection of time-integrated fluid fluxes from the literature. Grey area is the average regional pervasive flow-dominated flux estimated by Ague (1994a). Sources: (a) Breeding and Ague (2002), (b) Ferry (1992), (c) Ague (1994b), (d) Oliver et al. (1998), (e) Chamberlain and Rumble (1989). Range for (e) computed by Ague (2003) using average flux of 1.5×10 m^3 m^{-2} s^{-1} for 10^5 and 10^6 yr. (f) Ague (1994b), (g) Ague (1997), (h) Dipple and Ferry (1992), (i) Ferry (1992) and Léger and Ferry (1993), (j) Skelton et al. (1995), (k) Walther and Orville (1982) and Walther (1990). Range for (k) computed using total timescales of fluid flow of 10^6 yr and 10^7 yr. by Ague (2003), (l) Hanson (1997), (m) Evans and Bickle (1999). After Ague (2003).

exchange reactions or mineral-fluid reactions, yielding highly variable results. Time-integrated fluxes up to 10^6 m^3 of fluid/m^2 of rock have been estimated for pervasive flow through some contact aureoles and mid-crustal greenschist and amphibolite facies regional terranes. Values up to 10^9 cm^3 of fluid/cm^2 rock are reported for some metamorphic quartz veins. Walther and Orville (1982) calculated that fluid fluxes in a regional metamorphic terrane may reach 10^{-10} to 10^{-9} g/cm^2 sec, which is equivalent to 3 to 30 kg of fluid passing through each cm of crust above the 400°C isotherm during each million years of prograde metamorphism.

It seems fair to conclude that fluid infiltration is extensive in the Earth's crust, even in crystalline rocks with little obvious porosity. We are beginning to realize that the amount of fluid that passes through the crust is much greater than we had previously imagined. The ability of fluids to redistribute both heat and dissolved constituents in regional

and contact metamorphism means that fluids can profoundly affect the style of metamorphism, as well as the composition and texture of metamorphic rocks.

If we accept that fluid infiltration is readily achieved (if not pervasive), metasomatism becomes a question of relative mineral saturation and solubility in the flowing medium. We are already aware of the general aspects of fluid solutes from the discussion in Section 1.1. Transport of nonvolatile species is the result of the fluid dissolving and/or precipitating minerals as it moves through rocks. Because the chemical and physical environments change along the fluid path, the fluid must continually adjust to the changing conditions by re-equilibrating with the new mineral assemblages. This generally involves renewed dissolution and/or precipitation. Precipitation of vein quartz or carbonates from rising fluids in a fracture, or the development of metasomatic minerals, can be explained in this fashion.

2.2 J. B. Thompson's Metasomatic Column

J. B. Thompson (1959) proposed a hypothetical situation in the simple binary MgO-SiO_2 system consisting of a column of rock, one end of which consists of pure MgO (as periclase) and the other of pure SiO_2 (as quartz). The column between the two ends, he proposed, should have a *continuously varying bulk composition* from 100% MgO next to the periclase end to 100% SiO_2 (0% MgO) at the quartz end. To accomplish this, the proportions of periclase to quartz must vary progressively across the column.

Suppose next that this column is held at a temperature and pressure at which both forsterite and enstatite are stable in addition to periclase and quartz. Because the original MgO and SiO_2 are not stable together, they will react within the interior of the column to form enstatite and/or forsterite. At any particular point in the interior of the column, the stable mineral assemblage will reflect the initial MgO/SiO_2 ratio. As a result, three *interior* zones should develop (Figure 7):

1. A zone with periclase + forsterite, with the ratio of Per/Fo decreasing steadily from the pure-periclase rock (O% SiO_2) until a surface *F* is reached at which the proportion of periclase drops to zero and forsterite is 100%. Surface *F* marks the beginning of:
2. A zone with forsterite + enstatite. Across this zone Fo/En decreases steadily from zero En at surface *F* to 100% En at surface *E*, which marks the beginning of:
3. A zone of enstatite + quartz. Across this zone En/Qtz decreases steadily from zero % Qtz to 100% Qtz, from which point the rest of the column is pure quartz.

Note that the percentage of SiO_2 still increases steadily (and MgO decreases steadily) across the interior zones of Figure 7.

The concept of **local equilibrium** (Korzhinskii, 1959; J. B. Thompson, 1959) can be applied to this system. Note that the system as a whole is certainly *not* in equilibrium because it contains such incompatible phases as periclase and enstatite, as well as forsterite and quartz. Within any zone, however, the mineral assemblages are in *local* equilibrium because only compatible phases coexist in mutual contact. We can thus treat the rock column as a sequence of subsystems, each in local equilibrium as long as no incompatible phases are in direct contact.

Our column is not in local equilibrium, however, at surfaces *F* and *E*. Periclase in zone 1 is in contact with enstatite in zone 2 across surface *F*, and forsterite of zone 2 is in contact with quartz of zone 3 across surface *E*. As a result periclase + enstatite should react across surface *F* to form a thin monomineralic layer of forsterite. Similarly forsterite + quartz will react across surface E to form a thin layer of enstatite (Figure 8).

Once very thin layers of forsterite and enstatite form, local equilibrium reigns across the column because incompatible phases are no longer in direct contact anywhere. If diffusion permits, however, either through the crystals or some intergranular fluid, forsterite + quartz can still react across the monomineralic enstatite layer. This situation is analogous to the formation and growth of reaction rims and coronas.

As discussed above, diffusion is driven by chemical potential gradients across a medium. We can see in Figure 8 that the *content* of SiO_2 (and therefore also of MgO) is constant across the enstatite layer (pure enstatite is 59.8 wt. % SiO_2 and 40.1 wt. % MgO). The *chemical potential* of SiO_2 and of MgO, however, can vary in enstatite. To understand this, we refer to the phase rule. In a two-component system, such as in our rock column in Figure 8, a one-phase zone has $F = C - \phi + 2 = 2 - 1 + 2 = 3$ degrees of freedom. At a fixed temperature and pressure for the hypothetical example, $F = 1$. We can thus vary μ_{SiO_2} (or μ_{MgO}, but not both because they are related in enstatite at fixed *P* and *T*). In the two-phase assemblages, Fo + En

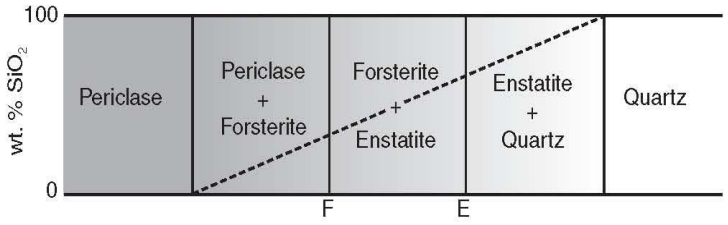

FIGURE 7 A hypothetical column of rock proposed by J. B. Thompson (1959). The left end is pure periclase and the right end pure quartz. Between these ends, the bulk composition varies continuously so that the wt. % SiO_2 increases linearly from left to right (dashed line).

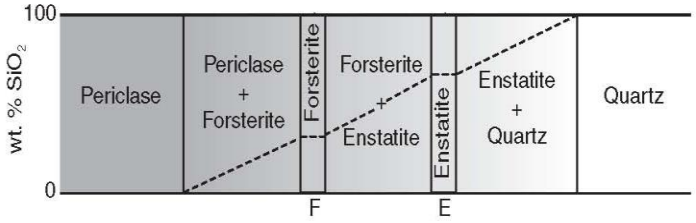

FIGURE 8 The hypothetical column of rock of J. B. Thompson (1959) after reactions create monomineralic forsterite and enstatite zones at F and E. The dashed line shows the variation in wt. % SiO_2 across the column. After Thompson (1959).

and En + Q on either side of the enstatite zone, the isothermal isobaric variance is zero $(F = 2 - 2 + 0 = 0)$, so that both μ_{SiO_2} and μ_{MgO} are fixed.

Perhaps the situation is more clear on a *G-X* diagram for a fixed *P* and *T* (Figure 9). This diagram is only schematic, but shows the general positions of the phases on such diagrams. For pure SiO_2 in a single-component system $(X_{MgO} = 0)$ because quartz is in its standard state (defined as the pure phase at the *P* and *T* of interest), μ_{SiO_2} is fixed at $\mu^{\circ}_{SiO_2}$, which is also G°_{Qtz}. Next, suppose MgO is mobile and progressively added to a quartzite. Migration of MgO into quartz gradually increases μ_{MgO}. Because quartz is stable, $\mu^{\circ}_{SiO_2}$, remains constant, but some MgO is present, presumably introduced along grain boundaries. When μ_{MgO} becomes great enough, a Mg-bearing solid phase will form. In the present case, the added MgO would react with some of the quartz to form enstatite.

It is a fundamental tenet of thermodynamics that, *at equilibrium, the chemical potential of any component is the same in all coexisting phases*. If this were not true (as mentioned earlier), the total free energy of the system could be lowered by having some component migrate from a phase with higher μ to a phase with lower μ until it reached the same value in both. Thus μ_{MgO} is the same in both quartz and enstatite (as is μ_{SiO_2}) once enstatite has formed and coexists with quartz. Their values can be determined by extrapolating the line connecting Qtz and En (Figure 9.) μ_{SiO_2} in both En and Qtz is equal to the intercept of theline at $X_{SiO_2} = 1\ (=\mu^{\circ}_{Qtz})$, and μ_{MgO} in each $(\mu^{En\text{-}Qtz}_{MgO})$ is equal to the intercept at $X_{SiO_2} = 0$. It may seem strange to speak of μ_{MgO} in quartz, but it does have a finite value. Because quartz admits a vanishingly small amount of MgO, μ_{MgO} increases *very* rapidly in quartz as X_{MgO} is increased in it. In other words, the energy of adding MgO to the quartz crystals is not favored, so that it takes only a minute amount of MgO in the presence of quartz to effectively saturate it, so that any excess MgO will go elsewhere (in this case, by reacting with some quartz to create enstatite). Also, the absence of a component in the solid rock does not mean that it may not have been abundant in a pore fluid phase.

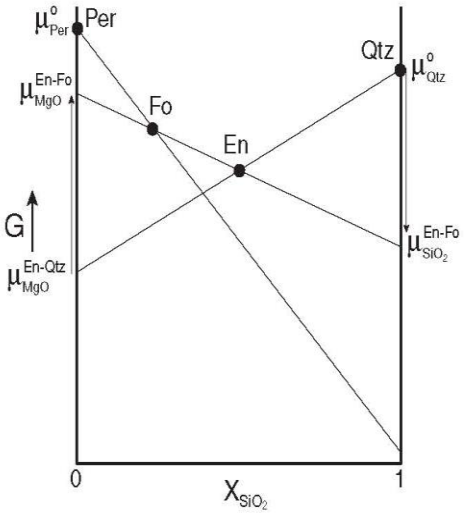

FIGURE 9 Schematic $G\text{-}X_{SiO_2}$ diagram for the SiO_2-MgO system at fixed temperature and pressure. See text for discussion.

Figure 9 agrees with our phase rule conclusion. At a particular value of *P* and *T* in the two-component MgO-SiO_2 system, coexisting En + Qtz is invariant and fixes (or buffers) both μ_{MgO} and μ_{SiO_2}. Suppose we continue to diffuse more MgO into our system. Quartz will continue to react with the added MgO until it is consumed. Although the amounts of quartz and enstatite vary during this process, μ_{MgO} and μ_{SiO_2} (the intensive variables) remain fixed. Once quartz is consumed, only En is present and μ_{MgO} and μ_{SiO_2} are free to vary. In this case, μ_{SiO_2} will now drop (because no quartz is left to fix it) and μ_{MgO} will rise until enstatite becomes effectively saturated in MgO and forsterite forms as any additional MgO reacts with the enstatite. Again we have two phases, and μ_{MgO} and μ_{SiO_2} are again fixed (or buffered) at $\mu^{En\text{-}Fo}_{MgO}$ and $\mu^{En\text{-}Fo}_{SiO_2}$ in Figure 9. Further addition of MgO will consume enstatite, after which μ_{MgO} can again rise in forsterite until periclase forms. A completely analogous argument can be made if SiO_2 is mobile and added to pure periclase at the opposite end of Figure 9 until forsterite, enstatite, and eventually quartz are formed.

Now let's return to our column in Figure 8 and address one of the incipient monomineralic zones, shown expanded in Figure 10. Because the proportion of Fo/En decreases toward the right across the two-phase Fo + En zone, X_{SiO_2} must correspondingly increase (and X_{MgO} must decrease). The same is true in the other two-phase zone as

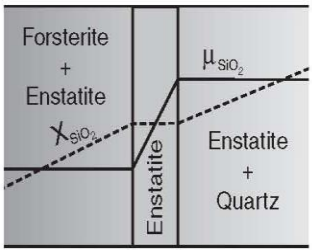

FIGURE 10 Expanded view of the monomineralic enstatite zone in Figure 8, showing the profiles of X_{SiO_2} and μ_{SiO_2}.

En/Qtz decreases. Within any one-phase zone both X_{SiO_2} and X_{MgO} are constant. The chemical potentials, however, behave differently. Because both two-phase assemblages buffer MgO and SiO_2, the chemical potentials are constant across these zones but are variable across the one-phase zone. The variation in X_{SiO_2} and μ_{SiO_2} is illustrated across Figure 10.

The difference in μ_{SiO_2} and μ_{MgO} across the monomineralic zone has the potential (so to speak) to drive diffusion across it. To the extent that diffusion is effective in the enstatite rock, SiO_2 and/or MgO can diffuse through it down their respective chemical potential gradients (only the SiO_2 gradient is illustrated in Figure 10). If only SiO_2 is mobile, it will diffuse through the En zone and react with forsterite at the far side to form enstatite, and the En zone will grow at the expense of the Fo + En zone. If only MgO is mobile, it will migrate through the En zone and react with quartz on the far side to form enstatite, and the En zone will grow at the expense of the En + Qtz zone. If both components are mobile, they will both diffuse through En in opposite directions, and the En zone will encroach upon both of the bimineralic zones on each side. One side may grow faster than the other, depending on the differences in diffusion coefficients for SiO_2 and MgO.

Because μ_{SiO_2} and μ_{MgO} are fixed on either side, as the width of the monomineralic zones expand, the gradients in μ become progressively less steep, and the driving force for diffusion drops correspondingly. This decrease in gradient may limit the growth of the zones. In mineral reaction rims and coronites diffusion commonly takes place through the lattice of a single-crystal rim. In many dry granulite facies rocks, an intergranular fluid is absent. In both situations diffusion is slow, and the monomineralic zones that form between reacting phases are typically less than a centimeter in thickness, which is apparently sufficient to inhibit further diffusion and growth. In contact metamorphic aureoles and rocks with a generous supply of fluids, diffusion may be much more efficient, either through a stationary fluid or assisted by infiltration, and metasomatic zones can be several meters thick.

Suppose diffusion in Thompson's hypothetical column is very efficient. The En and Fo zones may eventually grow to the extent that they completely replace the bimineralic zones. The column will then look like the one in Figure 11. The two-phase zones and smooth gradients in rock composition (expressed as wt. % SiO_2) in Figure 8 have been replaced by one-phase zones, smooth gradients in chemical potential, and abrupt changes in composition. *The reduction in the number of coexisting phases and the accompanying discontinuities in bulk composition (even where none existed before) are the hallmarks of metasomatic processes.* If the amount of periclase or quartz is limited, and metasomatism highly efficient, growth of the enstatite and forsterite zones may replace either phase entirely, resulting in a system composed of En + Fo, En + Qtz, or Fo + Per that is then in complete equilibrium (not just locally) because no incompatible phases occur anywhere in the system.

The reduction in the number of phases as components become mobile is what led Korzhinskii (1936, 1949, 1959, 1970) and Thompson (1959, 1970) to reformulate Gibb's phase rule to be applied to local equilibrium situations and to account for what Korzhinsikii called **"perfectly mobile" components**:

$$F = C - C_m - \phi + 2 = C_i - \phi + 2 \qquad (8)$$

where C is the total number of components, C_i is the number of "inert" components, and C_m is the number of "perfectly mobile" components. For each mobile component μ becomes controlled externally to the *local* system considered, in accordance with the notion of local equilibrium. Thus the variance is reduced by one in the local system for each such component. You may have encountered this concept in the

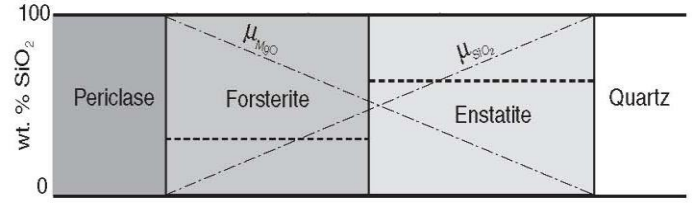

FIGURE 11 The hypothetical column of rock of J. B. Thompson (1959), with the sequences of mineral assemblages expected to form if diffusion is effective and the amounts of periclase and quartz prove inexhaustible. The dashed line shows the variation in wt. % SiO_2 across the column and the lighter dot-dashed lines show the variation in μ_{SiO_2} and μ_{MgO}. After Thompson (1959).

context of fluid components, such as mobile H_2O or CO_2. Now we recognize that it may be applied to any mobilized component. The "mineralogical phase rule" can be similarly modified if P and T are externally controlled:

$$\phi \leq C - C_m \text{ or } \phi \leq C_i \qquad (9)$$

This states that the number of minerals is reduced by one for each component that becomes mobilized, which is what we observed in J. B. Thompson's (1959) column above. If neither SiO_2 nor MgO is mobile, bimineralic zones remain. If either becomes mobile, monomineralic zones result. In the event that all components are mobile, we cannot have $\phi = 0$ (a void), so ϕ must equal at least one. Indeed, if everything is moving, it becomes impossible to prove that any one component did not move. This speaks to the problem of *reference frames*, discussed below. The local systems in Figure 11 are then generally monomineralic and $C_i = 1$ (the minimum number). At zone contacts μ_{SiO_2} and μ_{MgO} are buffered by the two phases in contact across the interface and thus internally controlled. On a local level C_m at a zone contact then equals zero and $C_i = 2$, so $\phi = 2$. As far as complete equilibrium is concerned, Figure 11 is not in equilibrium because the four phases, quartz, enstatite, forsterite, and periclase, are all present, and Per + En, Per + Qtz, and Fo + Qtz are all unstable associations. Only if the En and Fo zones expand to the point that Per and Quartz are exhausted will the column be in complete equilibrium. The concept of local equilibrium has the important attribute that we can apply equilibrium thermodynamics to any part of a larger disequilibrium system if the smaller part is itself in equilibrium. The larger system can then be treated as a **mosaic** of local equilibrium domains.

Vidale and Hewitt (1973) noted that "mobile" components need be able to move only to the extent that μ is controlled externally to the local system under consideration. Such components, they emphasized, may actually *move* less than some "inert" components. For example, if quartz is present in all the mineral assemblages of a system in an amount sufficient to internally control μ_{SiO_2}, then SiO_2 behaves as an inert component, even if it is soluble and easily moved. A particular component may behave as a mobile component in one occurrence and as an inert component in another, or even at different stages in the history of a single occurrence. To avoid inexorably relating external control invariably to high mobility, J. B. Thompson (1970) referred to Korzhinskii's "perfectly mobile" components as "*K*-components" and the "inert" components as "*J* components." Others refer to "perfectly mobile" components as "externally controlled" or "externally buffered" or "boundary value" components. Although some petrologists (e.g., Weill and Fyfe, 1964, 1967) justifiably criticize the Korzhinskii/Thompson phase rule [Equations (8) and (9)], the approach is effective in analyzing the broad characteristics of metasomatic rocks, and we shall adopt it in the discussions that follow. I shall also refer to externally controlled components as "mobile" because this is their usual and simplest behavior. We should be aware, however, of the term's limitations.

Because μ of mobile components are externally controlled intensive parameters of state, similar to pressure and temperature, their use as variables in phase diagrams can be very informative. In other words, because variations in μ for mobile phases, exerted from beyond the system, can exert some control on stable mineral assemblages, one can readily substitute μ as a variable for P or T in typical phase diagrams. Thus, instead of the P-T or T-X_{CO_2} diagrams with which you are by now so familiar, we could alternatively create T-μ diagrams, P-μ diagrams, or μ-μ diagrams (Korzhinskii, 1959). These differ from T-X or P-X pseudosections in that μ is an *intensive* variable and rigorously true for any phase or component in the plane of the diagram, whereas X is an *extensive* variable and the compositions of each phase must be projected onto the pseudosection.

Because, for any component i in phase A:

$$\mu_i^A = \mu_i^o + RT\ell n\, a_i^A$$

and because μ_i^o is a constant at any T and P, we can also substitute the *activity*, a_i (or preferably the log of a_i to maintain direct proportionality), for the chemical potential of any component in phase diagrams.

Figure 12 is a log a_{SiO_2} vs. log a_{H_2O} diagram for the MgO-SiO_2-H_2O system calculated at 600°C and 0.2 GPa using the TQW thermodynamic equilibrium program of Berman (1988, 1990, 1991). In the figure, I chose to add H_2O as an extra variable to determine its effect on the periclase–quartz column discussed above. Although the system is a three-component system, by making a_{SiO_2} and a_{H_2O} independent intensive variables, they may be treated as externally controlled and behave as though "mobile." The diagram is thus dominated by one-phase fields and not three-phase fields. The horizontal gray arrow in Figure 12 corresponds to a traverse across J. B. Thompson's column in Figure 11. At aqueous silica activities below $10^{-3.5}$ periclase is stable. As a_{SiO_2} increases to $10^{-3.5}$, $SiO_{2\,(aq)}$ reacts with periclase to generate forsterite. When a_{SiO_2} reaches $10^{-0.3}$, forsterite reacts with $SiO_{2(aq)}$ to generate enstatite. And quartz precipitates when a_{SiO_2} reaches $10^{0.0}$, or 1.0, meaning that the solution is now saturated in silica. Of course a_{SiO_2} cannot become larger than 1.0 because the fluid is saturated and any additional SiO_2 simply precipitates as more quartz.

If a_{H_2O} is raised, periclase gives way to brucite (Per + H_2O = Bru) at low a_{SiO_2}. Raising a_{SiO_2} at high H_2O activities (just below water saturation) then traverses the forsterite field (2 Bru + $SiO_{2\,(aq)}$ = Fo + 2 H_2O) and the talc field (3 Fo + 5 $SiO_{2\,(aq)}$ + 2 H_2O = 2 Tlc), until quartz precipitates. Increasing a_{SiO_2} at $a_{H_2O} = 10^{-0.5}$ in Figure 12 results in the sequence Per → Fo → En → Tlc → Qtz. The En-Tlc boundary corresponds to the reaction 3 En + 2 $SiO_{2(aq)}$ + 2 H_2O = 2 Tlc. Figure 12 not only quantifies the Thompson column approach, but introduces alternative columns as well.

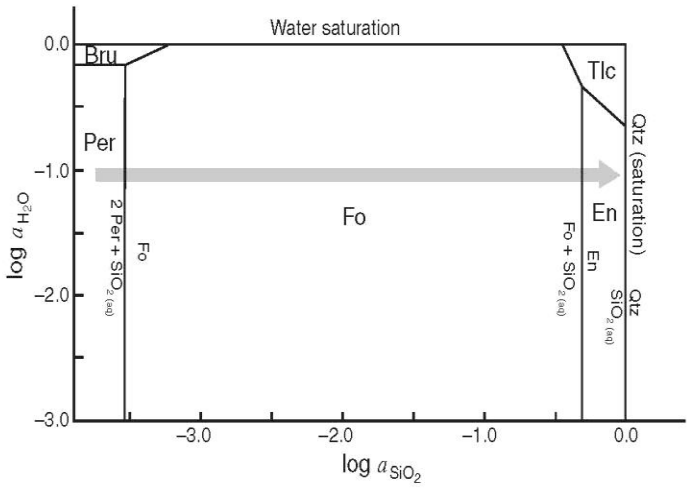

FIGURE 12 a_{SiO_2}– a_{H_2O} diagram for fluids in the MgO-SiO_2-H_2O system at 600°C and 0.2 GPa calculated using the TQW program (Berman, 1988, 1990, 1991).

μ-μ or log a-log a diagrams are superior to the common chemographic diagrams when treating systems with several mobile components, as discussed by Brady (1977). A compatibility diagram, such as a triangular SiO_2-MgO-H_2O diagram, assumes that all components are immobile and that most common compositions on the diagram are represented by three-phase assemblages. Even if H_2O is mobile, a SiO_2-MgO compatibility diagram (Figure 13) suggests that two-phase assemblages are the norm. One-phase assemblages only occur when the composition is equal to that of one of the phases (and gives the impression that this is a rather fortuitous situation). Figure 9 shows that one-phase assemblages may be expected when SiO_2 and/or MgO become mobile, which agrees with Figure 12.

In light of the previous discussion involving metasomatism in a hypothetical column of rock, let's summarize how diffusion and infiltration might operate during mass transfer and effect changes in the composition of rocks. In purely diffusional metasomatism the components diffuse through the rock, either through crystals or between them, most effectively through a stationary intergranular fluid medium. In purely infiltrational metasomatism, a solution flows into a rock and permeates the rock along a network of pores. If the solution is not in equilibrium with the new host rock, it reacts with the rock, exchanging components with the solid phases until local equilibrium is attained (or at least approached). As the fluid moves, it carries solute species and continuously exchanges them with successive rock volumes that it encounters, commonly producing different reactions at different zones of the flow.

Korzhinskii (1970) derived transport equations for both the diffusion and infiltration models and used them to analyze qualitatively the development of metasomatic zones. On the basis of his models he proposed that purely diffusive and infiltrative metasomatism are similar in a number of respects. For example, both produce a sequence of zones with a reduced number of phases, and the zones are typically separated by sharp metasomatic "fronts" (if local equilibrium prevails). On the other hand, diffusion and infiltration may potentially be distinguished on the basis of the following distinctive features (Korzhinskii, 1970; Hofmann, 1972):

- Infiltration can produce much wider zones than diffusion alone. The diffusion zones are commonly measured on the centimeter scale or less, whereas infiltration can produce zones several meters across.
- Diffusion can lead to reactions between rock components and diffusing components, but direct precipitation of a mineral cannot occur by diffusion in one direction because components migrate to areas of reduced activity. Infiltration can result in precipitation.
- Minerals within a zone can vary in composition as a result of diffusion because μ_i can vary steadily across a zone. μ_i is more constant within a zone during infiltration, so that the composition of resulting minerals that exhibit solid solution tends to be nearly constant.
- In infiltration, all components migrate in the same direction. In diffusion, different components can migrate in opposite directions (as J. B. Thompson's bimetasomatic column above). Bimetasomatic diffusion can result in the precipitation of new minerals.

Remember that diffusion and infiltration are simply end-member processes and that metasomatism in nature may consist of varying proportions of fluid motion (infiltration) and diffusion of solute species through that fluid, or diffusion from the fluid into the rocks through which it flows. "Wall–rock metasomatism" is a typical example of the combined process in which solutions percolate along a fracture (infiltration), and dissolved constituents diffuse from the fracture into the wall rocks through a largely stationary intergranular pore fluid.

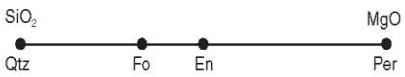

FIGURE 13 SiO_2-MgO chemographic diagram assuming only Qtz, Fo, En, and Per are stable.

2.3 Changes Associated with Metasomatism

Once we begin to treat metamorphism and metamorphic reactions as involving fluids and potential dissolved species, it becomes possible to balance mineral reactions in several possible ways. For example, in addition to the tremolite → diopside reaction:

$$\mathrm{Tr} + 2\,\mathrm{Qtz} + 3\,\mathrm{Cal} = 5\,\mathrm{Di} + 3\,\mathrm{CO_2} + \mathrm{H_2O}$$

We could balance the reaction in, among other ways, the following:

$$\mathrm{Tr} + 6\,\mathrm{H^+} = 2\,\mathrm{Di} + 3\,\mathrm{Mg^{2+}} + 4\,\mathrm{SiO_{2(aq)}} + 4\,\mathrm{H_2O} \quad (10)$$

$$\mathrm{Tr} + 2\,\mathrm{Ca^{2+}} = 4\,\mathrm{Di} + \mathrm{Mg^{2+}} + 2\,\mathrm{H^+} \quad (11)$$

$$\mathrm{Tr} + 2\,\mathrm{SiO_{2(aq)}} + 3\,\mathrm{Ca^{2+}} + 2\,\mathrm{H_2O} = 5\,\mathrm{Di} + 6\,\mathrm{H^+} \quad (12)$$

etc.

The reaction that occurs depends on the physical conditions, as well as the nature of the fluid and its solute content. In infiltration, the latter may depend on the nature of the rock through which the fluid most recently passed. In addition to *P* and *T*, then, the reaction may be dependent on pH and the activities of Ca^{2+}, Mg^{2+}, and SiO_2, etc. in the fluid. Determining which reaction occurred in situations with component mobility requires good petrography, including careful examination and interpretation of textures, accurate modes across isograds or metasomatic fronts, and an adequate reference frame.

The **reference frame problem** can be illustrated by returning to the metasomatic column of J. B. Thompson (1959). Remember from Figure 10 that the monomineralic enstatite zone can grow at the expense of the Fo + En zone on the left if SiO_2 is mobile, or it can grow at the expense of the Q + En zone if MgO is mobile. Alternatively, the En zone can expand in both directions at different rates if MgO and SiO_2 are both mobile, but to different extents. In natural situations of metasomatism that occur across ultramafic–quartzo-feldspathic contacts, for example, it may be difficult to determine which way a metasomatic front moved and what rock was replaced by a particular zone. Brady (1975) discussed the problem of reference frames in diffusional processes. The usual choice is a tacit assumption that diffusion takes place in reference to a single fixed point, which is really equivalent to a reference frame consisting of several points, all in fixed positions relative to each other. Because volume changes are common in metasomatic processes, such a choice of reference frame is impossible, and the extent of diffusion for various components, if so referenced, cannot be realistic. Brady (1975) reviewed several alternative reference frames. A common approach in experimental investigations and quantitative models of metasomatism is to choose some weighted average of the determined velocities of all chemical components, such as the motion of the center of mass. Alternative reference frames of this type may include assuming a fixed mean number of moles of all components, a fixed mean volume or mass, or that some individual component is fixed or immobile.

The reference frame problem is closely related to the problem of determining exactly what chemical changes occurred to produce a metasomatic rock in the field. Suppose we have an ideal situation in which we can determine the original contact (perhaps because some immobile residue was left, such as a layer of graphite, or rutile grains), and we thus know which rock was replaced. Furthermore, suppose we have an essentially unaltered sample of the replaced rock some distance from the metasomatized contact zone (similar to the periclase or quartz zones at the ends of our hypothetical column above). If we compare the chemical composition of the initial and altered rock, we may be tempted to conclude that any constituents that decrease from the initial analysis to the final one were removed, and those that increase were added. This has an implicit assumption, however, that the total mass of the sample hasn't changed. Recall that the meaning of "percent," as in "wt. %," implies that 100 g of the sample is essentially constant, and that the parts that make up those 100 g are simply exchanged through the walls surrounding the 100-g sample, picogram-for-picogram, so that the total remains the same. When matter is in flux, however, several alternative scenarios are possible. Perhaps material was only added during metasomatism, which diluted all of the non-added components. Comparing analyses on a wt. % basis would give the false impression that the diluted components *decreased* because they would have smaller percentages in the analysis of the altered rock than in the original. Alternatively, material may only have been removed, giving the false impression that the conserved constituents increased on a percentage basis, even though they never really moved. This problem is another aspect of the "closure problem".

Gresens (1967) provided an approach for comparing two chemical analyses that attempts to solve the closure problem in certain cases. He provided a set of equations that allows calculation in terms of initial and final rock analyses and assumptions concerning either the volume change or the gain or loss of any one component. Gresens' (1967) equations have the form:

$$d_i = \left(f_v \frac{g_B}{g_A} c_i^B - c_i^A \right) \quad (13)$$

where d_i is the amount of component i gained or lost, A is the original unaltered rock and B is the altered equivalent, c_i is the concentration of i (wt. %) in rock A or B, and g is the specific gravity or density. f_v is the volume factor, the number by which the total volume of the initial rock should be multiplied to result in the volume of the final rock. Although intended for volume changes, the equation is entirely general. If we wish to retain a weight basis, rather than a volume basis, f_v may be replaced by f_m, a mass factor, and the specific gravities may be ignored. In that case we would be dealing with changes in mass during metasomatism and not changes of volume.

As an example of his approach Gresens (1967) compared two rocks, from the Stavanger region of Norway, the analyses of which are given in Table 1. Rock A is a garnet phyllite, and rock B is an albite porphyroblast schist,

interpreted as being derived from A by metasomatism. Figure 14 is a diagram of the net gains or losses of the oxides (d_i) versus the volume factor (f_v) using Equation (13) and specific gravities of 2.838 for the original phyllite and 2.777 for the altered schist.

A vertical line at $f_v = 1.0$ in Figure 14 is equivalent to assuming that volume is constant and intersects the oxide curves at values that are equivalent to simply subtracting the wt. % oxide values in column B of Table 1 from those in column A (with a volume weighting factor equal to the specific gravity ratio applied). Thus SiO_2, Na_2O, and CaO are added, and the other major oxides are lost during metasomatism if it is considered a constant volume process. Figure 14 also shows comparisons using alternative volume change interpretations. For example, if $f_v < 0.6$ (the volume loss is such that the final rock B is less than 60% of the volume of the original rock A), all of the constituents could have been removed in different (but specific) proportions and still produce rock B from rock A. If $f_v > 1.6$, on the other hand, all of the constituents could have been added. There is no textural basis for making a choice among these alternatives because the rocks are deformed, but the usual "choice" of constant mass (equivalent to direct comparison of the analyses) now seems as arbitrary as any alternative. A choice of constant volume may seem the most natural because we may not expect substantial volume changes in a rock at depth, but if matter is in flux, and the rocks are being deformed, there may be no compelling argument to support this contention. If rock A is neatly pseudomorphed during alteration, one may make a reasonable case for a constant volume process, but otherwise not.

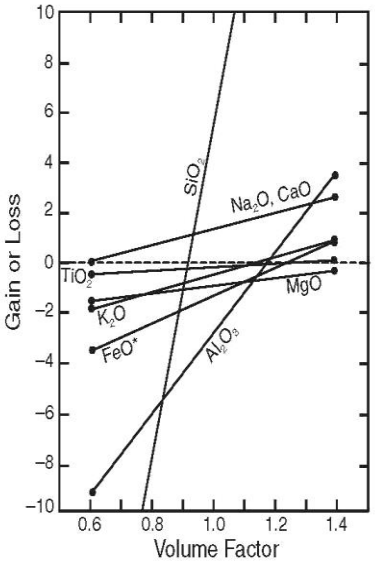

FIGURE 14 "Gresens-type" variation diagram showing the gains or losses (in grams per 100 grams of original rock A) as a function of the volume factor, f_v, in Equation (13). Rock A is a garnet phyllite from Stavanger, Norway, and rock B is a metasomatized albite schist, supposedly derived from (A). After Gresens (1967). Copyright © with permission from Elsevier Science.

TABLE 1 Analyses of Two Rocks from the Stavanger Region, Norway

Oxide	A	B
SiO_2	60.6	64.7
TiO_2	0.80	0.59
Al_2O_3	18.5	15.45
FeO*	6.84	5.41
MgO	2.42	1.48
MnO		
CaO	1.66	2.92
Na_2O	1.81	3.09
K_2O	4.02	3.46

A good alternative to assuming constant volume, however, may be indicated in Figure 14. Note that the Al_2O_3 and TiO_2 curves both intersect the $d_i = 0$ value (no gain or loss) at about the same value of f_v (about 1.2). Al and Ti are considered to be among the least mobile elements during metamorphism. Perhaps their mutual intersection with $d_i = 0$ indicates an appropriate choice for a volume change consistent with Al-Ti immobility. Such a choice of $f_v \approx 1.2$ (about 20% volume increase) also correlates well with minimal gain or loss of Fe and K. If we choose such a volume change, a vertical line at $f_v = 1.2$ yields corresponding gains or losses of all the oxides. Using this choice we see that SiO_2, Na_2O, and CaO are again the only oxides gained, but FeO* and MgO are all that is lost. The gain in SiO_2 is substantial, but correlates with the high solubility of SiO_2 in aqueous solutions.

Grant (1986) developed an alternative approach to the Gresens (1967) diagram, in which he rearranged Gresens' equations into a linear relationship between the concentration of a component in the altered and original rocks. In a plot of the concentrations of each component in the initial unaltered rock versus the concentration of those same components in the altered rock (Figure 15), any line that connects the origin with a point representing the concentration of any single component in both rocks can be called an **isocon** (constant concentration). An isocon for constant Al_2O_3 has been drawn in Figure 15. Such a line represents all points for which the concentration of a component in the altered rock (C^A) equals 0.835 times the concentration of the same component in the original unaltered rock (C_o). Note that the points for K_2O, FeO, MgO, and TiO_2 all fall near this line, correlating to the similar intersection of these oxide lines in Figure 14. The isocon with slope of 1.0 corresponds to $C^A = C_o$, and hence no mass gain or loss. Points above this are components gained during constant mass alteration, and those below the line are lost (again in agreement with Figure 14). Grant's (1986) isocon diagrams are easier to construct and solve, but they are still based on the same criteria developed by Gresens (1967).

The approaches of Gresens (1967) and Grant (1986) underscore the closure problem and the arbitrary nature of our common practice of comparing directly the analyses of altered rocks with their presumed unaltered parent rock. In

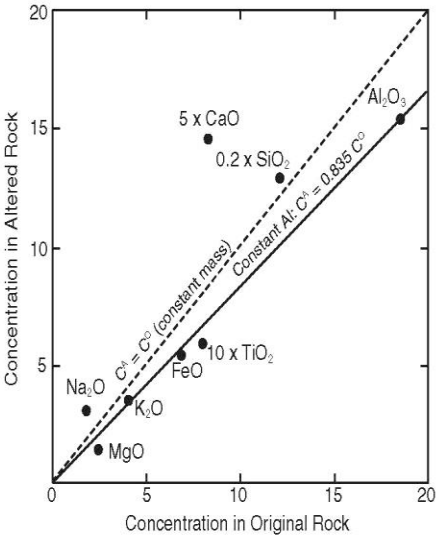

FIGURE 15 Isocon diagram of Grant (1986) for the data from Table 1. Some oxides have been scaled to provide a better distribution of data points.

some cases these approaches may indicate a preferred alternative, and the changes may be normalized to values consistent with minimal changes in elements regarded as immobile during metamorphism. The Gresens–Grant approaches may be strengthened if trace elements are added, and typically immobile elements such as Zr and Y, etc. also intersect the $d_i = 0$ curve close to the point at which Al and Ti do. The mobility of an element commonly varies with the conditions, rocks, and fluids involved. Al, for example, is generally regarded as an element of low solubility in metamorphic fluids, and of limited mobility under most metamorphic conditions. In low-to-medium grade metamorphosed ultramafic rocks, however, few Al-bearing minerals are stable, and Al may be quite mobile. If I were to apply the Gresens/Grant approach, I would keep an open mind and critically evaluate the patterns, with obvious emphasis on which elements intersect $d_i = 0$, and where they do so. The approach should complement good petrographic work, however, and not be a substitute for it.

Further discussion of metasomatism and the formation of metasomatic zones from a theoretical perspective becomes somewhat abstract. I think that it is far better to discuss the methodology by using some real examples. We shall thus address the two most common metasomatized rock types: ultramafics and calcareous skarns. Other types certainly occur, including fenites, greisens (fluorine and hydrothermal alteration of granitoids), rodingites (Ca metasomatism of mafic rocks associated with ultramafics), etc., but the two following examples will suffice to illustrate the approaches and processes involved.

2.4 Examples of Metasomatism: Ultramafics

Metasomatic zones occur commonly at the margins of pod-like ultramafic bodies in regional metamorphic terranes. Because of sharp initial chemical contrasts across the contact between the ultramafic and the (commonly) pelitic or quartzo-feldspathic country rock, sharp chemical potential (or activity) gradients in SiO_2, MgO, FeO, etc. are common and diffusion or infiltration may result. Descriptions of metasomatic ultramafic bodies date at least back to Gillson (1927), Read (1934), and Phillips and Hess (1936).

The number of low-ϕ zones that develop at metasomatized ultramafic margins, as well as their thickness and mineralogy, depends upon the stability of the various minerals and the ability of the components to migrate. These, in turn, depend upon the *P-T* conditions, the composition of the juxtaposed rocks, and the nature and mobility of the fluid phase. Because ultramafic rocks correspond closely to the MgO-FeO-SiO_2 system, the mineralogy of the ultramafic is typically relatively simple (≤ 3 principal phases). When any of these components become "mobile," according to Equation (9) the number of phases (ϕ) is reduced by the number of "mobilized" components. As a result, monomineralic and bimineralic zones are common.

Read (1934) described several types of mineral zonation around small (a few centimeters to 7 m in length) ultramafic pods in pelites in the Shetland Islands that were metamorphosed first in the biotite to kyanite zones and then affected by later chlorite zone retrograde metamorphism. He described an "ideal" zonation in the area as having a serpentine core with successive concentric zones of nearly monomineralic talc, actinolite, chlorite, and biotite as illustrated in Figure 16. Carbonate and Fe-Ti oxides are common minor phases. The zones are typically a few cm in width. The dark chlorite and micaceous zones were called **blackwall** zones by early talc miners and quarrymen in the northeastern United States, and the term is now commonly used more loosely by petrologists to refer to nearly any zone that forms around metasomatized ultramafic bodies.

Variations on Read's ideal sequence are consistent with more advanced chemical migration (and/or smaller bodies), which causes some zones to grow at the expense of other

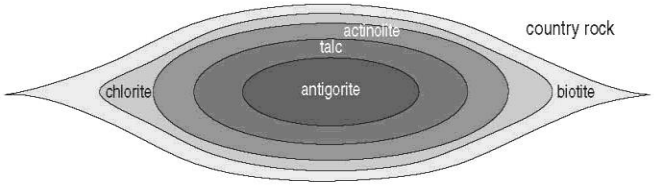

FIGURE 16 "Ideal" mineral zonation due to metasomatism in < 3-m-long ultramafic pods in low-grade regionally metamorphosed pelites at Unst, Shetland Islands. After Read (1934).

zones, eventually consuming them. This process was described above in conjunction with J. B. Thompson's hypothetical column, in which the forsterite and the enstatite zones grew to the extent that they consumed adjacent zones. Read (1934) described at least the following variations:

core →			**rim**
Atg	Tlc	Act	Bt
Tlc	Act	Bt	
Tlc	Act	Chl	Bt
Tlc	Chl	Bt	
Act	Bt		

but several monomineralic pods in the area, such as biotite, chlorite, or actinolite clots, may also represent metasomatized ultramafics.

Phillips and Hess (1936) described similar zoned ultramafic bodies from the Appalachians, some extending several hundred meters in length. They also noted variations in zonation, similar to those of Read (1934), and concluded that two main types of ideal zonation occur there, a low-temperature zonation:

core →		**rim**	**country rock**
Atg	Tlc + Mgs	Tlc	Chl | quartz-mica schist

and a high-temperature zonation:

core →		**rim**	**country rock**
Atg	Tlc + Mgs	Act	Bt | pelitic schist

The authors noted that chlorite occurs at the Act-Bt boundary in several high-temperature bodies and attributed it to retrograde alteration. Chlorite, however, is stable up to 600 to 700°C, so it may be part of the high-temperature equilibrium assemblage, as it was considered by Read (1934).

Carswell et al. (1974) described symmetrically zoned *veins* in peridotite in the high-temperature gneisses of southern Norway. They noted the sequence:

country rock →		**vein center**
Peridotite	En	Ath | Tr | Chl

This type of occurrence is distinctive in being not only higher grade but associated with the introduction of components via alkali–halide-rich aqueous fluids along fractures in the host peridotite (~90% olivine, 10% enstatite). (I reversed the center-margin sequence above to conform left → right to the petrology of the other sequences.)

Matthews (1967) found pods in the Lewisian gneisses on the Isle of Skye that are similar to those of Read (1934). The ultramafic core has been entirely replaced by talc-carbonate, which is rimmed by an actinolite and a biotite zone. The absence of a chlorite zone is probably due to higher metamorphic grade at Skye. Sharpe (1980) described the following zonation in an ultramafic rock in the quartzofeldspathic gneisses of southwestern Greenland:

core →			**rim**	**country rock**
Atg	Tlc	Act	Hbl | Chl	q-feld. gneiss

Fowler et al. (1981) described the zones developing about small serpentine–magnesite "balls" in gneissic country rocks that conform to the following common sequence:

core → rim				**country rock**
Atg + Mgs	Tlc	Act	Hbl | Chl	q-feld. gneiss

Pfeiffer (1987) described several types of zonation, both around ultramafic bodies and as veins in ultramafic rocks in the high-grade Valle Verzasca region of the Swiss Alps. Many of the zoning patterns are similar to those described above, but some are complex.

Sanford (1982) examined 40 to 50 ultramafics in New England and studied 4 in detail (in the greenschist and amphibolite facies). He found the following zonal sequence to be common:

core →				**rim**
⟨um⟩	Tlc + Carb	Amph + Chl	Chl | Trans	CR

The ultramafic (um) assemblage was antigorite in the greenschist facies, and olivine + talc in the amphibolite facies. The country rock (CR) was generally a biotite-bearing mafic rock, more pelitic in some cases. The transitional-to-CR zone was commonly a biotite + amphibole ± plagioclase ± epidote zone.

Zone boundaries in most metasomatically zoned ultramafics are fairly abrupt, as the mineralogy changes quickly, but there is typically some overlap between phases. For example, Read (1934) described the transition between the talc and actinolite zones as one in which the amount of actinolite increased and the amount of talc decreased across a short distance. Similarly, the chlorite content increased within the actinolite zone as the chlorite zone was approached.

Sanford (1982) supplied sufficiently detailed descriptions to construct modes along a traverse. His traverse at the Grafton talc quarry in Vermont is shown in Figure 17. The zones at Grafton are:

A	B	C	D	E
Tlc + Ath	Tlc	Act + Chl	Trans	CR

Zone A is the main ultramafic body, and zone E is the quartzo-feldspathic country rock (CR). Note in Figure 17 that none of the zones is perfectly monomineralic. Curtis and Brown (1969) attributed the overlap of mineral types to kinetic effects, in that the reaction rate is unable to keep pace with diffusion or infiltration. In addition, the number of phases typically decreases progressively as the number of components that are mobilized increases. It has been noted in several experimental columns in which metasomatic fluids have been introduced that the number of phases decreases from the unaltered rock toward the source of infiltrating fluids, reflecting more elemental mobility in the fluid-rich domains. In cases of bimetasomatism, there is typically a single phase at the initial contact, where μ gradients are steepest, and increasing numbers of phases in both directions from that point. These trends conform to Korzhinskii's (1959, 1970) theory of metasomatic zoning. Regardless of the overlap of minerals in the observed traverses, the trends

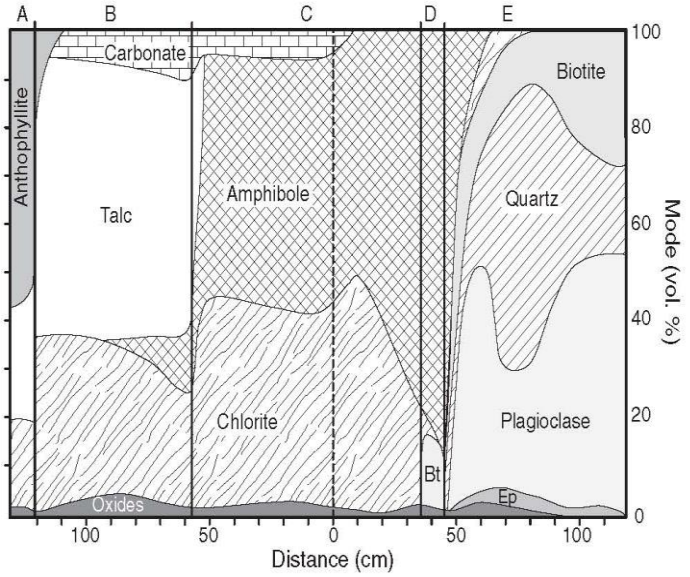

FIGURE 17 Variation in mineral proportions across the zones between the ultramafic and quartzo-feldspathic gneiss contact at Grafton, Vermont, after Sanford (1982). Zone letters at the top correspond to the zones listed in the text. Zone letters at the top are: A = Tlc + Ath, B = Tlc, C = Act + Chl, D = transitional, E = quartzo-feldspathic country rock. The vertical dashed line represents the estimated initial contact. After Sanford (1982). Reprinted by permission of the *American Journal of Science*.

toward developing a sequence of zones, each dominated by one or two principal phases, is still clear.

As Brady (1977) pointed out, diffusion in simple two-component systems, such as in the J. B. Thompson column above, can be uniquely modeled in terms of the ideal sequence of mineral zones that form because the variation in composition is a one-dimensional function of the ratio of the two components. Systems with three components or more, however, even if only one component is mobile, can have a number of possible zonal sequences. The mineral assemblages that form, and their sequence, depends not only on the amount of mobile component(s) added or lost, but also upon their ratio and the ratio of "immobile" components at any point along the column. It is thus impossible to predict a single zonal sequence. As is so commonly the case, a theoretical approach is best used to analyze what *has* happened at a given locality, rather than to attempt to predict what *should* happen.

H_2O and CO_2 are clearly mobile in most ultramafic systems and are involved in the mineralogy of several zones. H_2O is typically present in sufficient quantity that it establishes a constant value of μ_{H_2O} within any zone and is rarely buffered by the local mineral assemblages. CO_2 may be buffered by serpentine + talc + magnesite, but carbonate only occurs in an inner talc + magnesite zone. We can avoid complexity by considering the chemical potentials of H_2O and CO_2 to be constant and use variations in μ_{MgO} and μ_{SiO_2} (ignoring carbonates) as a first approximation in attempting to develop a model for the formation of ultramafic metasomatic zones that reproduces the types observed above.

At a constant temperature, pressure, μ_{H_2O}, and μ_{CO_2}, the minerals present in the low-temperature types of zones, such as that of Read (1934), can be represented on an *AMS* diagram, in which $A = Al_2O_3$, M = MgO + FeO, and $S = SiO_2$ (Figure 18). Points X and Y in Figure 18 indicate the bulk composition of the serpentinite and the pelitic country rocks, respectively. Again, because more than one component is involved, there is no single path between X and Y that is universally applicable and that would provide a unique solution to the development of a sequence of mineral zones. For example, if SiO_2 is the only diffusing component, then the sequence might be:

(1) Atg | Tlc | Ms + Chl | CR (Qtz-Ms schist)

In this case, shown as the two vectors labeled 1 in Figure 18, composition Y loses SiO_2 as composition X gains SiO_2. The loss of SiO_2 from Y (Ms + Chl + Qtz) results in Ms + Chl in the adjacent zone, and the gain in SiO_2 to X (Atg) results in the formation of Tlc. Note that because one component is mobile in the pseudo-three-component *AMS* diagram shown, three-phase assemblages do not occur (except at zone boundaries). Thus only two-phase assemblages (represented by successively encountered tie-lines) and one-phase assemblages (points) are to be found within

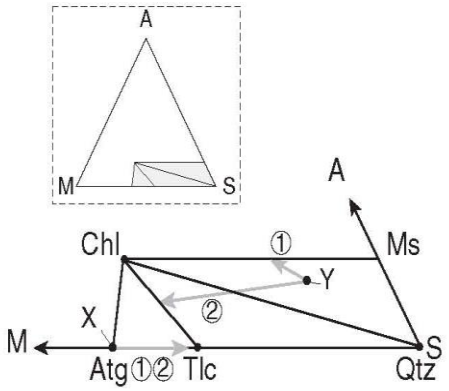

FIGURE 18 *AMS* diagram (A = Al_2O_3, M = MgO + FeO, and S = SiO_2), projected from K_2O, for ideal lower-temperature metasomatic zones around ultramafic bodies. After Brady (1977).

the metasomatic zones. Note that the sequence in Figure 18 is actually Atg → Atg + Tlc (at the contact or across a short interval) → Tlc.

Alternatively, M may be mobile, so that X loses M, and Y gains it (vectors 2 in Figure 18), resulting in this possible sequence:

(2) Atg | Tlc | Tlc + Chl | Chl + Qtz | CR (Qtz-Ms schist)

Figure 19 is a qualitative $\mu_M - \mu_{SiO_2}$ diagram (M = MgO + FeO) showing the two sequences above and the sequence observed at low temperatures by Phillips and Hess (1936). Path 2, for example, follows the Atg + Chl boundary, to the Tlc + Chl boundary, to the Qtz + Chl boundary, to the Chl + Ms + Qtz point (pelitic country rock). Note that the Atg, Tlc, and Qtz saturation surfaces buffer the fluid composition, so that μ_M and μ_{SiO_2} must vary in sympathy, even though only one species may be "mobile." For the observed sequence of Phillips and Hess (1936), the fluid composition leaves the saturation surfaces in the monomineralic chlorite zone and cuts through the Chl field, requiring that both M and SiO_2 be diffusing components.

By projecting from K_2O in Figure 18, we have ignored its importance as a diffusing component. It may play a role, but the major mineral zones can be derived without addressing it. Aluminum is also assumed to be immobile in balancing the reactions to create this $\mu-\mu$ diagram (Figure 19). At higher temperatures, actinolite and biotite are important phases. The role of biotite is similar to that of chlorite in the treatment just described. Actinolite requires CaO, which is presumably derived from the country rocks and must diffuse through the biotite and actinolite zones in order for actinolite to form.

Figure 20 shows the positions of analyzed rocks (large dots) from the Shetland Island zones of Read (1934), reported by Curtis and Brown (1969). The analyses match

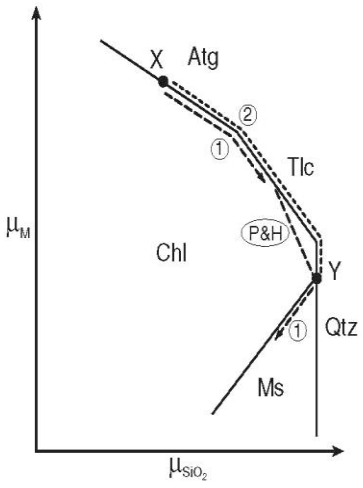

FIGURE 19 Hypothetical $\mu_M - \mu_{SiO_2}$ diagram for fluids in the *AMS* system (Figure 18). Paths (1), (2), and (P&H) refer to the theoretical paths in Figure 18, and the observed sequence of Phillips and Hess (1936). After Brady (1977). Copyright © with permission from Elsevier Science.

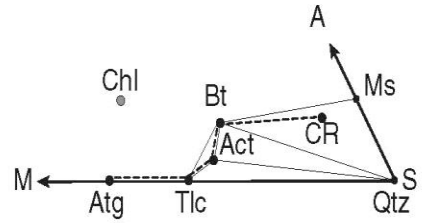

FIGURE 20 The same portion of the *AMS* diagram as in Figure 18, projected from K_2O and CaO, with the locations of analyzed rocks (large dots) from the metasomatized zones of Read (1934; see Figure 15), reported by Curtis and Brown (1969). The dashed curve represents a path through the zonal sequence. After Brady (1977). Copyright © with permission from Elsevier Science.

closely the ideal mineral compositions for monomineralic zones. The dashed curve represents a pathway corresponding to the sequence of zones in Figure 16. If chlorite is not a retrograde product in the Shetland rocks, the path must divert drastically from the actinolite zone rocks back to the chlorite zone and back again to the biotite zone. Remember, however, that the process is driven largely by chemical potential or activity gradients of species in the fluid, and these may not necessarily be directly proportional to the bulk rock compositions. It is thus possible to have reversals in the composition of components in the bulk rock along a traverse. It is also possible to have peaks or reversals in some, but not all, activity gradients in a system with several diffusing species. We will see some more well-constrained examples of these features in the following section on calc-silicate skarns.

In his detailed study in New England, Sanford (1982) noted that the composition of several phases varied significantly across zones (noted earlier as more compatible with diffusion than with infiltration). He also placed the initial contact at or near the actinolite–chlorite boundary because both Cr and Ni (typically immobile and concentrated in ultramafic rocks) decrease drastically from this point toward the quartzofeldspathics. Assuming that Ni and Cr are immobile, he calculated estimates for the volume change at three localities, concluding that the altered ultramafic zones increased in volume (from 1.4 to as much as 11 times, but remember that they are thin) and that the country rocks decreased in volume. Of course these factors change if Cr or Ni moved. On the basis of reaction textures and the mineral modes, combined with inferred displacement of zone contacts, Sanford also estimated the reactions and component fluxes associated with metasomatism of the ultramafics and country rocks. Figure 21 illustrates the reactions and fluxes estimated for the Grafton quarry, corresponding to the mineralogy shown in Figure 17. Note from the proposed fluxes at the top of the figure that every major oxide was to some extent mobile. The major fluxes were of Si from the country rocks into the ultramafic and of Mg from the ultramafic to the country rocks. The other fluxes were of lesser magnitude (with the possible exception of CO_2). Note that Al, commonly regarded as relatively insoluble and immobile, was mobile at Grafton (as in most metasomatized ultramafics).

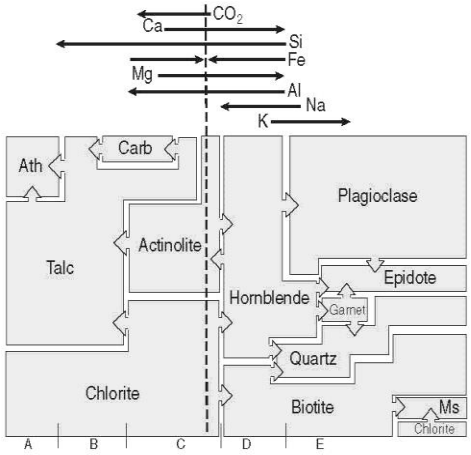

FIGURE 21 Schematic representation of major silicate mineral reactions and component fluxes associated with metasomatism of the ultramafic body at Grafton, Vermont. Elemental fluxes across various zones are indicated by the arrows at the top. Arrows between mineral boxes (somewhat distorted from the true modes in Figure 16) indicate reactions. When horizontal, these arrows involve metasomatic reactions; when vertical they are approximately isochemical. The zones listed at the bottom correspond to those in Figure 16, and the heavy dashed line is the estimated original contact. After Sanford (1982). Reprinted by permission of the *American Journal of Science*.

Sanford (1982) was able to calculate the chemical potentials of most major elements at several points along the traverses at four of his zoned ultramafic bodies. This is possible at points where sufficient phases were present to buffer μ of a particular component at a given temperature and pressure. For example, remember from J. B. Thompson's column illustrated in Figure 10 that μ_{SiO_2} is buffered by either two-phase assemblage (Fo + En or En + Qtz), but is variable across one-phase zones. Thus Sanford (1982) could constrain the μ of several species when the number of phases was high and the variance therefore low: typically at zone boundaries. Figure 22 shows the results of his calculations for the Grafton locality. Any migrating component should move from zones of high μ toward areas of lower μ. Again, note the locally steep gradients in SiO_2 and MgO. Na_2O migrated from the quartzo-feldspathic country rock toward the ultramafic. FeO migrated from both rock types toward the contact zone at Grafton, but only into the ultramafic at the other three localities studied by Sanford. CaO has a high μ in the actinolite zone and decreases toward the country rocks (it is a minor component and unconstrained in the ultramafic body). CaO thus migrated from the ultramafic body to the country rocks. Al_2O_3 shows some interesting peaks and troughs. Assuming that the migration of all species reflects a coherent flux between only two initial contrasting rock types, the peaks and troughs in the profiles of Al_2O_3 and FeO indicate that these components migrated *up* their μ gradients at several points on a local basis. Such "uphill" migration has been discussed by Cooper (1974) and is attributed to interactions between diffusing components. The flux of some major component may stabilize a phase that acts as a "sink" for a less mobile or less abundant component, so that the lesser component becomes concentrated. Conversely, a phase that acts as a "sink" for a lesser component may not be stable due to the fluxes of more dominant components, resulting in local depletion of the lesser component. It follows that "uphill" migration is limited to local effects on less plentiful or mobile elements, and it cannot occur in simple binary systems, but requires several components.

The approach of studying metasomatic rocks by a combination of standard chemographic diagrams linked with chemical potential or activity profiles and μ-μ or log *a*-log *a* diagrams has proved fruitful and could be applied to the higher-temperature ultramafic reaction zones as well. Rather than risk overdoing it, we will move on and show how the technique can be applied to another common metasomatic rock type, calcareous skarns.

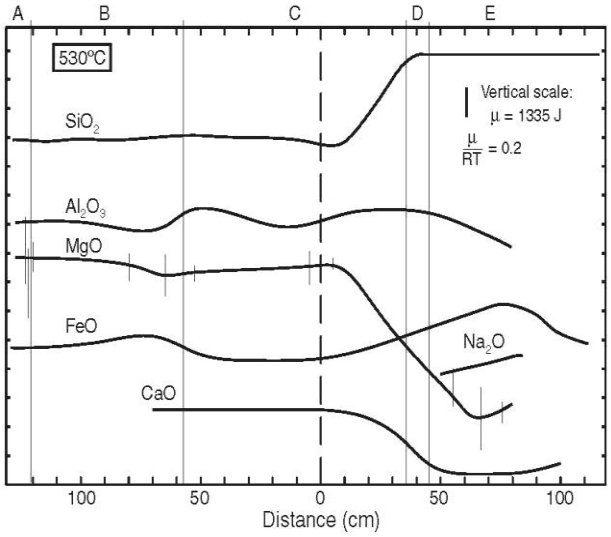

FIGURE 22 Variation in chemical potentials of major components across the metasomatic zones at Grafton, Vermont. Estimated temperature = 530°C. Typical data points and error bars are illustrated for the MgO profile. Lettered zones at the top correspond to those in Figure 16. The dashed vertical line is the estimated original contact. After Sanford (1982). Reprinted by permission of the *American Journal of Science*.

2.5 Examples of Metasomatism: Calcareous Skarns

A **skarn** (or **tactite**) is a rock dominated by Ca-Fe-Mg-rich calc-silicate minerals, usually formed by replacement of carbonate-bearing rocks during either regional or contact metamorphism. Although recrystallization of sufficiently impure carbonate rocks can produce a skarn, most are created by metasomatism, either bimetasomatism across the contact between unlike lithologies or infiltration of silica-rich fluids into carbonate rocks. Some investigators prefer to restrict skarns to include only the replacement types, but this makes it hard to identify a skarn without correctly interpreting its genesis. Others use the term more generally, encompassing a number of replacement rocks, including ultramafic blackwalls, but most investigators prefer restricting it to calc-silicate rocks that replace carbonates. Einaudi et al. (1981), in their extensive review, further subdivided skarns into magnesian skarns (that replace dolomite), calcic skarns (that replace calcite), and various ore skarns (particularly common are magnetite and tungsten–scheelite ore skarns).

Alternatively, skarns can be subdivided on the basis of their geologic setting (Kerrick, 1977), as illustrated in Figure 23. **Magmatic skarns** are found at the contact between igneous rocks (usually granitoid plutons) and marbles. **Vein skarns** form along fractures or small dikes in marbles. Infiltration is a dominant process in skarn formation of these two types. **Metamorphic skarns** form at the contact between carbonate and silicate lithologies, usually representing original sedimentary layers, but also including chert nodules in marbles, etc. Diffusion (usually bimetasomatism) directly between the contrasting rock types is usually the dominant process involved in the generation of metamorphic skarns. Vein skarns and magmatic skarns usually involve infiltration, but it may be accompanied by diffusion. These skarns form by metasomatism and are usually only a few centimeters thick. All three of these occurrence types are also possible in ultramafic and other metasomatic rocks. The examples of ultramafic blackwalls above were predominantly metamorphic, but some vein types were also described. Magmatic types are more dramatic for skarns than for other rock types because of the radical compositional contrast between a silicate magma, commonly releasing acidic aqueous solutions, and a carbonate country rock.

Skarns are typically zoned, and the zones have a reduced number of phases, as we would expect when components make the transition from "inert" to "mobile" states. As in zoned ultramafics, the mineralogy, thickness, and number of zones depends upon the *P-T* conditions, the composition of the juxtaposed rocks, and/or the nature and mobility of the fluid phase. Table 2 illustrates some types of zonation observed in selected examples of skarns described in the literature. Magmatic and metamorphic types are ordered toward the marble on the right; vein types are listed from the center of the vein to the marble margin (again on the right), having a symmetric other half not shown. The minerals within a zone, when reported, are listed in order of decreasing abundance. The list is by no means comprehensive, and I have left out many variations in the interest of brevity, tending to select the more complex zonation when more than one type was described in any particular work. Higher degrees of mobility tend to simplify the zonation and replace adjacent zones, imparting less information. Table 2 merely illustrates a spectrum of the possible types of zoning. Magmatic skarn zones are not to be confused with contact metamorphic isograds and the zones between them. The zones in Table 2 are due to metasomatic addition of material by diffusion and/or infiltration, and are much smaller than most contact metamorphic aureoles, which are largely thermal effects (and may or may not have some accompanying metasomatism).

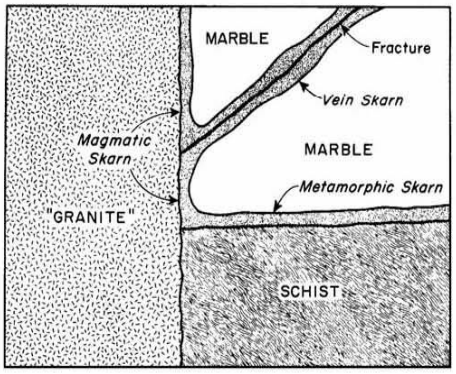

FIGURE 23 The three principal types of skarns. From Kerrick (1977). Reprinted by permission of Oxford University Press.

Note in some magmatic examples in Table 2 that an **endoskarn** develops within the plutonic rock. Although metasomatism associated with plutons is usually dominated by the infiltration of the carbonate country rocks by fluids released by the cooling pluton, an endoskarn may form when CaO and/or CO_2 migrate back into the igneous body, causing hornblende or biotite to dehydrate and alter to pyroxene. Endoskarns are readily recognized in the field by the gradual transformation of the black igneous mafics to green pyroxene. When endoskarns are present, the term **exoskarn** is commonly used to distinguish the more typical skarns that form outside the contact by replacement of the country rocks.

It is well beyond our scope here to attempt to explain the development of every zonal sequence in skarns, even those listed in Table 2. It will suffice for our present purposes to model a typical example or two, so that we might see how our approach can be used to understand calc-silicate mineral zonation in general.

The simplest chemical system in calc-silicate skarns is an initial calcite-quartz contact ($CaO\text{-}SiO_2\text{-}CO_2$), an excellent example of which is Joesten's metasomatized chert nodules in marbles in the Christmas Mountains of southwestern Texas (Joesten, 1974, 1991; Joesten and Fisher, 1988), one of which is shown in Figure 24. At a given μ_{CO_2}, metasoma-tism between the chert and carbonate is a matter of diffusion in a binary system of either CaO into the nodule or SiO_2 outward, or both. At the very high temperatures in the inner aureole of the gabbro body in the area, wollastonite is stable, as are the unusual high-temperature calc-silicate minerals tilleyite, spurrite, and rankinite. Joesten noted that the nodules developed a series of monomineralic

TABLE 2 Some Examples of Metasomatic Zones Developed in Calc-Silicate Skarns

Zones	Type	Width	Reference
Diorite (Hbl+Plag) | Endoskarn (Cpx+Plag) | Pyroxene (Cpx) | Garnet (Grt+Cpx) | Marble (Cal)	Magmatic	3 cm	Kerrick (1977)
Dior.? | Endoskarn (Plag+Grt+Ep) | Garnet (Grt+Cpx+Ep) | Pyroxene (Cpx+Grt+Ep) | Marble (Cal)	Magmatic	6 cm	Kerrick (1977)
" | Endoskarn (Plag+Ep+Cte+Di) | Garnet (Grt+Cpx+Qtz) | Wollastonite (Wo) | Marble (Cal+Cpx +Ep+Grt)	Magmatic	5 cm	Kerrick (1977)
Garnet (Grt+Qtz) | Wollastonite (Wo+Qtz) | Marble (Cal)	Vein	2 cm	Kerrick (1977)
Amphibolite (Plag+Hbl) | Ep-Trem (Ep+Tr+Plag) | Pyroxene (Cpx+Ep) | Garnet (Grt+Cpx) | Marble (Cal)	Metamorphic	1.5 cm	Kerrick (1977)
Hornfels (Bt+Kfs +Plag) | Pyx-Plag (Cpx + Plag) | Pyx-Ep (Cpx+Ep +Plag) | Garnet (Grt + Cpx) | Woll. (Wo) | Marble (Cal+Qtz +Grt)	Metamorphic	2 cm	Kerrick (1977)
Pelite (Bt+Ms+Qtz) | Amphibole (Qtz+Plag +Amph+Kfs) | Pyroxene (Cpx+Plag) | Garnet (Grt+Cpx) | Marble (Cal+Cpx +Wo)	Metamorphic	7 cm	Thompson (1975)
Pelite (Bt+Kfs +Plag+Qtz) | Amphibole (Amph+Kfs +Plag) | Pyroxene (Cpx+Kfs +Plag) | Garnet (Grt + Pyx) | Marble (Cal+Wo +Grt)	Metamorphic	4 cm	Jamtveit *et al.* (1992)
Pelite (Qtz+Bt+Feld) | Diopside | Garnet | Wollastonite | Marble (Cal)	Metamorphic		Brock (1972)
Granite (Hbl+Bt+Plag +Kfs+Qtz) | Garnet (Grt+Wo) | Pyroxene (Cpx) | Pyx-Mont (Cpx+Mtc) | Ol (Fo+Mtc) | Marble (Cal+Fo)	Magmatic	10 cm	Tilley (1951b)
Quartz | Wollas-tonite | Rankinite | Spurrite | Tilleyite | Marble (Cal)	Metamorphic (chert nodule)	1-2 cm	Joesten (1974)
Quartz | Tremolite | Calcite | Marble (Dol)	Vein	1 cm	Walther (1983)
Cal + Di | Cal + Tr + Di | Cal + Tr | Calcite | Marble (Dol)	Vein	< 15 cm	Bucher-Nurminen (1981)
Cal + Tr | Cal + Fo + Tr | Cal + Fo | Marble (Dol+ Cal + Fo)	Vein	< 15 cm	Bucher-Nurminen (1981)
Cal + T + Di | Cal + Tr + Phl | Cal + Tr | Cal +Fo | Marble (Dol+ Cte + Fo)	Vein	< 15 cm	Bucher-Nurminen (1981)
Cal + Di | Cal + Tr + Di | Cal + Fo | Cal + Atg + Fo | Marble (Dol)	Vein	< 15 cm	Bucher-Nurminen (1981)
Cal + Tr + Phl | Cal + Tr + Tlc + Phl | Do + Cal + Tr + Phl | Marble (Dol)	Vein	< 15 cm	Bucher-Nurminen (1981)
Q. Diorite | Silica-Enriched | Endoskarn (Czo + Plag) | Pyrox. (Cpx+Tr) | Forsterite (Cal + Fo) | Marble (Dol)	Metamorphic	3.5 cm	Frisch and Helgeson (1984)
(same) | Pyrox. (Cpx+Tr) | Antigorite | Forsterite (Cal + Fo) | Marble (Dol)	Metamorphic	3.5 cm	Frisch and Helgeson (1984)
Czo | Di + Tr + Czo + Chl | Pyrox. (Cpx) | Antigorite | Forsterite (Cal + Fo) | Marble (Dol)	Vein	1.5 cm	Frisch and Helgeson (1984)

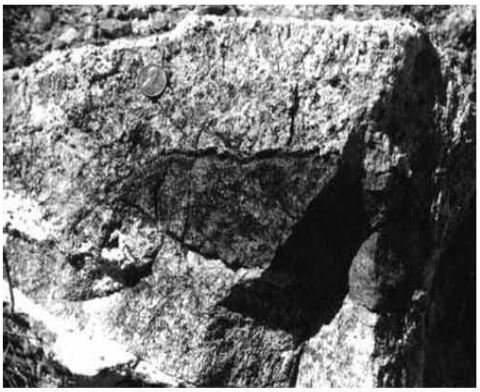

FIGURE 24 Chert nodule in carbonate with layer sequence: calcite|tilleyite|wollastonite|quartz. Christmas Mountains, Texas. From Joesten and Fisher (1988). Copyright © The Geological Society of America, Inc.

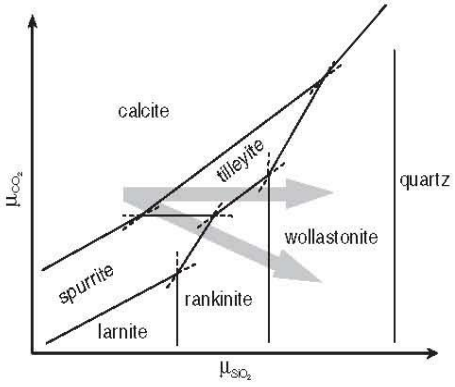

FIGURE 25 Schematic isothermal isobaric $\mu_{CO_2}-\mu_{H_2O}$ diagram for fluids in the $CaO\text{-}SiO_2\text{-}H_2O$ system at high temperatures. After Joesten (1974). Reprinted by permission of the *American Journal of Science*.

marginal layers that he attributed to diffusion both of CaO into the nodule and SiO_2 outward (bimetasomatism). The mineralogy of the layering depends on the temperature (the proximity to the gabbro contact) and the extent of diffusion (the progress of replacement reactions as zones grow). Among the more complex zonal patterns between the marble and the chert nodule core, listed in order of distance from the contact in meters, are:

distance	**rim → core zonation**
0–5 m:	Cal | spurrite | rankinite | Wo | Qtz
0–16 m:	Cal | tilleyite | spurrite | rankinite | Wo | Qtz
16–31 m:	Cal | tilleyite | Wo | Qtz
31–60 m:	Cal | Wo | Qtz
> 60 m:	Cal | Qtz

Figure 25 is a $\mu_{CO_2}-\mu_{SiO_2}$ diagram Joesten (1974) used to explain the development of the zones. μ-μ diagrams are relatively easy to construct if the reactions are known because the slope of any reaction boundary is simply the ratio of the stoichiometric coefficient of the abscissa component divided by that of the ordinate component as they are involved in the reaction (Korzhinskii, 1959). For example, the spurrite–rankinite reaction can be expressed as:

$$\underset{\text{spurrite}}{3\,Ca_5Si_2O_8CO_3} + 4\,Si = \underset{\text{rankinite}}{5\,Ca_3Si_2O_7} + 3\,CO_2 \qquad (14)$$

The slope is thus +4/3 (positive because CO_2 and SiO_2 are on opposite sides of the reaction). The tilleyite to rankinite reaction is:

$$\underset{\text{tilleyite}}{3\,Ca_5Si_2O_7(CO_3)_2} + 4\,SiO_2 = \underset{\text{rankinite}}{5\,Ca_3Si_2O_7} + 6\,CO_2 \qquad (15)$$

so the slope is only +4/6 (or 2/3). Using these slopes and the Schreinemakers approach, we can create Figure 25 if the stable phases are known. Note that the sequence:

Cal | tilleyite | rankinite | Wo | Qtz

also described by Joesten, can be created by increasing the chemical potential of SiO_2 (or decreasing that of CaO in this simple binary system) at constant μ_{CO_2} along the horizontal gray arrow in Figure 25. This is analogous to the process of SiO_2 diffusing into the marble from the chert, or of CaO diffusing into the nodule from the carbonate. Joesten proposed that spurrite develops by subsequent dehydration of tilleyite at its interior margin to produce the sequence described between 5 and 16 m from the contact above. Alternatively, CO_2 may have decreased as SiO_2 increased (sloping gray arrow in Figure 25) to develop the sequence directly. Joesten (1974) and Joesten and Fisher (1988) proceeded to use quantitative models of diffusion and growth to predict the sequence of zones that formed over time and the migration of zone boundaries as one mineral zone replaces another. Remember from the J. B. Thompson column that a zone, such as the enstatite zone in Figure 10, may grow at the expense of forsterite on the left if SiO_2 is more mobile and at the expense of quartz on the right if MgO is more mobile. Modeling which boundary moves in a given situation requires quantitative models based on realistic diffusivities (see below).

As discussed above, for systems with multiple components there may be several diffusing constituents. No single unique path is implicated because several components may migrate, and one cannot determine their interactions *a priori* (Brady, 1977). Modeling the zonal sequences in more complex skarns in systems including CaO, SiO_2, MgO, Al_2O_3, and K_2O is thus more complicated and variable, typically involving both multimineralic and monomineralic zones.

For example, A. B. Thompson (1975) described the zonal sequence listed in the seventh row in Table 2,

which developed at the contact between interbedded pelite and carbonate layers in a roof-pendant of metasediments in Vermont. Figure 26 is an ACF diagram (projected from K_2O) showing the location of the minerals in the various zones and the trace of whole-rock compositions between adjacent pelite and calcite marble. Remember (in contrast to the application of such diagrams in normal usage), when elements are "mobile," three-phase assemblages tend to be less common than two-phase (tie-line) assemblages or one-phase assemblages. The ideal sequence, if two-phase assemblages predominate, can be determined by the successive tie-lines intersected by a straight line from the pelite (Shale) to the carbonate (Cal) in Figure 26:

pelite (Ms, Bt, An) | An + Hbl | Hbl + Czo | Czo + Cpx | Cpx + Grt | Ves + Cpx | Cal

This sequence, however, is not unique. Although CaO appears to be most mobile, and the traverse from the pelite to the carbonate appears to be dominated by an increase in CaO, the A/F ratio need not be constant and may be controlled by phases stabilized by varying μ_{CaO}. Note that the sequence of analyzed bulk-rock compositions follows a zigzag curve in Figure 26 that includes some one-phase (Cpx) and three-phase (Grt + Cpx + Czo) assemblages. It is a common feature of metasomatic zones that the bulk rock composition varies in such an irregular fashion. Remember, smoother chemical gradients in the more mobile components, typically in the *fluid phase*, drive the reactions, causing the rock compositions to conform to the extent that they can, given the limited mobility of other components. Alternative sequences may avoid Grt and Ves between the Cpx zone and the marble, or they may cross Grt + Ves instead of Ves + Cpx. There is no way to predict which will occur from Figure 26 alone.

Figure 27 is a diagram developed by Frantz and Mao (1979) for the CaO-MgO-SiO_2-CO_2-H_2O (CMS-CH) system that shows the composition of the solute species in the H_2O-CO_2 fluid that is in equilibrium with several common calc-silicate phases. Because experimental mineral–fluid solution data are not yet available, the diagram is only schematic. This diagram is similar to a ternary $\mu_{CaO}-\mu_{MgO}-\mu_{SiO_2}$ diagram (or log a equivalent) because μ-μ and activity diagrams, such as Figures 12, 19, and 25, refer to the chemical potential of components in the *fluid* phase. Again, because components are mobile, the number of phases is reduced, and because more than two components are involved, no unique path between any two points is predetermined. The fluid is always approaching equilibrium with the solid mineral assemblage, which may also buffer the fluids. If quartz and a dolomitic marble are initially in contact, a number of paths are possible between the quartz and dolomite fields in Figure 26, each representing a different sequence of zones.

For example, the direct path (a) in Figure 27 would produce a sequence of metasomatic zones:

(a) Qtz | Tr | Fo | Dol

Alternatively, paths (b) and (c) may occur if the solids buffer the fluid and two-phase zones are stabilized, resulting in the following sequences:

(b) Qtz | Tlc + Tr | Tr + Fo | Fo | Fo + Cal | Dol

(c) Qtz | Di + Tr | Tr | Tr + Cal | Cal + Dol | Dol

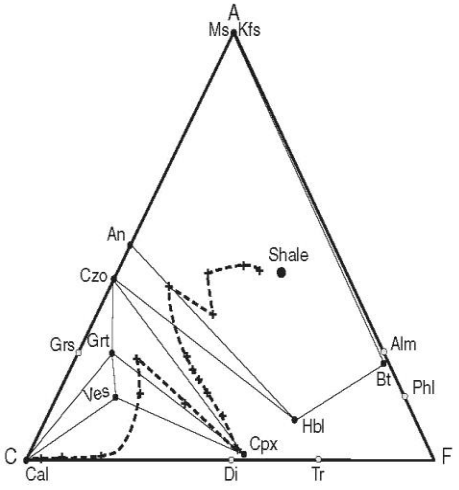

FIGURE 26 Al_2O_3-CaO-(FeO + MgO) diagram (projected from K_2O), showing the mineral phases and calculated bulk compositional path for metasomatic zones that develop at the contact between pelitic and carbonate layers near Lake Willoughby, Vermont. Ideal mineral compositions are in gray, real ones in black. After A. B. Thompson (1975). Reprinted by permission of Oxford University Press. Plus signs represent analyzed bulk-rock compositions within zones.

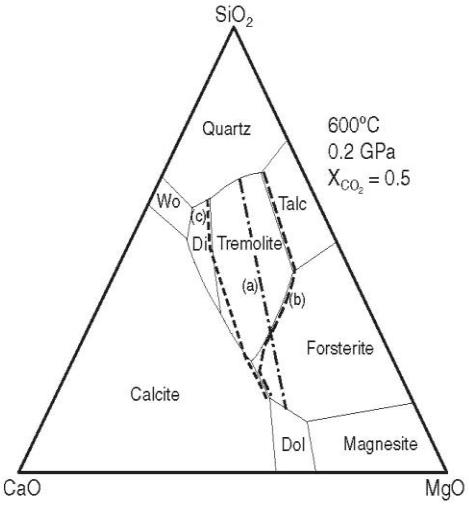

FIGURE 27 Schematic CaO-MgO-SiO_2-CO_2-H_2O diagram, showing the composition of the fluid solution in equilibrium with the phases shown at approximately 600°C and 0.2 GPa (projected from H_2O and CO_2 at a constant 1:1 ratio). After Frantz and Mao (1976). Reprinted by permission of the *American Journal of Science*.

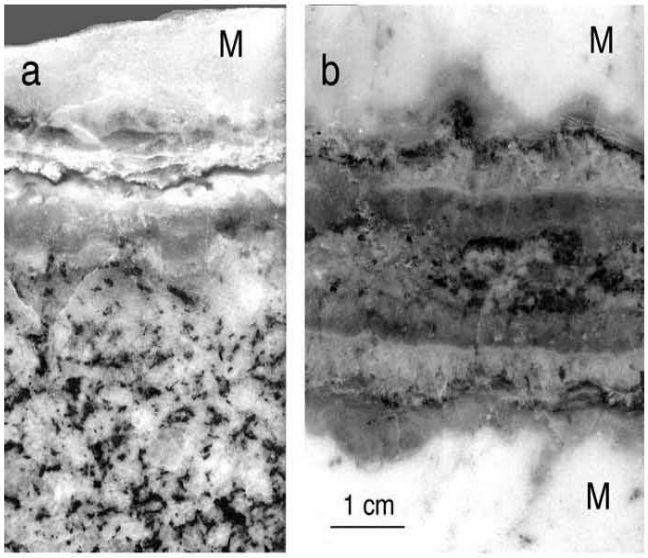

FIGURE 28 (a) Metasomatic zones separating quartz diorite (bottom) from marble (top). Zonation corresponds to the third row from the bottom in Table 2. (b) Symmetric metasomatic vein in the dolomite. Zonation corresponds to the last row in Table 2. Adamello Alps. After Frisch and Helgeson (1984). Reprinted by permission of the *American Journal of Science*. Photos courtesy of Hal Helgeson.

Some of these paths correspond to sequences observed in nature. [Note the similarity to some of the sequences described by Bucher-Nurminen (1981) in Table 2.] Numerous other paths involving monomineralic and bimineralic zones are also possible in Figure 27, involving wollastonite or talc as well as the phases listed above.

I present one final example because of its careful mineralogical control and theoretical treatment. Frisch and Helgeson (1984) described several zoned skarns, including magmatic and vein types, that develop in dolomitic marbles in the Adamello region of the Italian Alps. Figure 28 shows two samples, one at the contact between quartz diorite and marble, and the other a vein within the marble. Both samples illustrate the marked zonation typical of metasomatized rocks. Figure 29 shows how the mineralogy of the rocks varies along a traverse across the zones of the magmatic quartz diorite–dolomite contact corresponding to the sample shown in Figure 28a. As in the ultramafic examples discussed above, careful petrography reveals that the zones are not monomineralic, but usually mixtures of two or more minerals, reflecting varying degrees of component mobility. Note also that the quartz diorite is also altered to an endoskarn of tremolite, calcite, muscovite and clinozoisite.

Frisch and Helgeson (1984) considered several models for the development of the metasomatic zones in both the magmatic and vein occurrences and attempted material balance calculations for various reference frames (Section 2.3) based on each model. Models include (1) reciprocal diffusion (bimetasomatism) between the units, (2) infiltration of fluid from the pluton into the marble, (3) infiltration of both units by a fluid entering along a contact fissure, and (4) infiltration of fluid along the contact fissure accompanied by diffusional transfer into the units. Frisch and Helgeson concluded that model (4) conformed best to the geological and material balance constraints, and that the metasomatic zones at the igneous contact are thus really postmagmatic metamorphic, or even vein-type skarns.

On the basis of the mineral assemblages, Frisch and Helgeson (1984) concluded that the conditions of metamorphism were in the vicinity of 425°C and 50 MPa. The occurrence of clinozoisite + quartz requires that X_{CO_2} in the fluid is about 0.02 or less. They calculated log a-log a

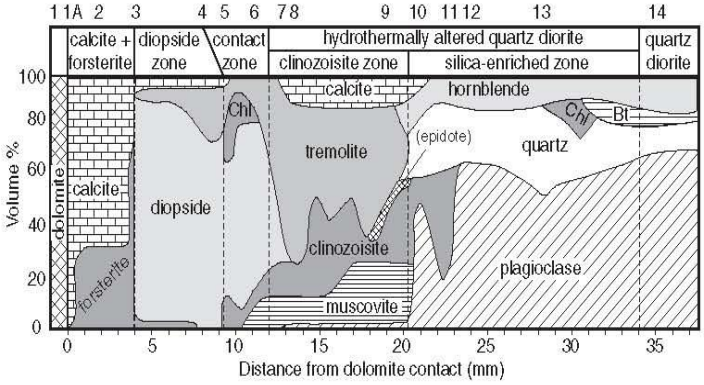

FIGURE 29 Mineral zones and modes developed at the contact between quartz diorite and dolomitic marble in Figure 28a. Initial contact may be at either side of the contact zone. Index numbers at the top indicate the locations of bulk chemical analyses. After Frisch and Helgeson (1984). Reprinted by permission of the *American Journal of Science*.

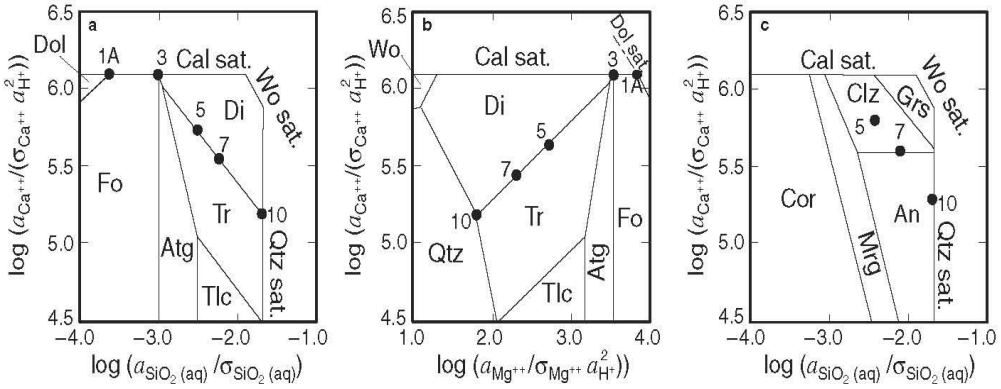

FIGURE 30 (a) log a_{CaO} − log a_{SiO_2} and (b) log a_{CaO} − log a_{MgO} diagrams in the system CaO-MgO-SiO_2-H_2O-CO_2. (c) log a_{CaO} − log a_{SiO_2} diagram for the same system + Al_2O_3, all at 425°C, 0.05 GPa, and X_{CO_2} = 0.007. Numbered points correspond to the index numbers in Figure 29. After Frisch and Helgeson (1984). Reprinted by permission of the *American Journal of Science*.

diagrams for fluids in equilibrium with various minerals. Such log a diagrams are quantitative and can be calculated using the thermodynamic computer program SUPCRT92 (Helgeson et al., 1978; Johnson et al., 1992).

Figure 30 illustrates Frisch and Helgeson's (1984) log a_{Ca}–log a_{SiO_2} and log a_{Ca}–log a_{Mg} diagrams. In an attempt to be as rigorous as possible, the expression for the activity of a solute species i with charge z is modified by dividing by σ_i, a factor to account for solvation, and a_H^z to account for hydration (Walther and Helgeson, 1980). Bowers et al. (1984) published a compendium of such activity diagrams for use in analyzing systems involving equilibrium among minerals and aqueous solutions. The traverse of index numbers at the top of Figure 29 corresponds to the partial list of numbered dots in Figure 30, in which point 1A represents Cal + Dol + Fo equilibrium at the marble boundary, point 3 = Cal + Fo + Di, points 5 and 7 = Di + Tr, and point 10 represents quartz saturation in equilibrium with tremolite within the quartz diorite. In the Al-bearing system of Figure 30c, the occurrence of clinozoisite is shown at points 5 and 7, and An + Qtz is shown at point 10.

Note from Figure 30 that fairly large changes in the interstitial fluid are responsible for the mineralogy of the various zones and that the gradient of points in Figure 30a changes abruptly at the mineral zone boundary, consistent with buffering of activities at boundaries and variation across the boundaries between the buffered points (as in Figure 19).

Unlike infiltration of H_2O or CO_2, the nonvolatile migration and zoning seen in ultramafic blackwalls and skarns is rare over large distances and uncommon even over small distances. Conditions favoring mobilization of nonvolatile components include high temperatures, strong μ gradients, the presence of saline (generally chloride) aqueous fluids, and high permeability. For multicomponent systems, simple profiles of bulk rock composition along a traverse are generally irregular and will not directly indicate the metasomatic process, which involves gradients of dissolved species in a fluid phase. Calculating chemical potential or log activity diagrams for solute species, as constrained by the mineral buffering assemblages (usually at zone boundaries where more phases coexist), provides much better indicators of the processes involved.

2.6 Quantitative Models and Experiments of Metasomatism

Several investigators have attempted to develop quantitative models of diffusion, infiltration, or combined processes based on mobile component concentrations and the extent of the mobility of each. The mathematics is complex and I consider these models beyond the scope of this book (and of my poor brain). Modern models expand upon Korzhinskii's (1959, 1970) initial theories and attempt to predict not only the fluxes, but also the widths of the metasomatic zones and the reactions by which they grow as zone boundaries migrate in one direction or another. For an excellent review, see Zaraisky (1993). Numeric solutions based on local equilibrium models include the infiltration models of Hofmann (1972), Fisher (1973), Lichtner (1985), and Lichtner et al. (1986); the diffusion model of Weare et al. (1976); and the combined diffusion–infiltration models of Frantz and Mao (1976, 1979) and Fletcher and Vidale (1975). Joesten and Fisher (1988) applied a diffusion model to the development of the monomineralic zones around the chert nodules discussed above. The growth of reaction rims and coronas is an identical diffusion-controlled process, and the theory can be applied to their growth as well. Zaraisky (1993) praised the "macrokinetic" model (Balashov and Lebedeva, 1991) as the current culmination of treating metasomatic zonation in terms of local equilibrium and thermodynamics of reversible reactions, combined with a kinetic description of the approach toward those limits. Given initial and boundary conditions, they developed a set of differential equations that attempts to fully describe the structure of a zoned metasomatic column, with local equilibrium as a limiting case.

The Russians are presently the experts in experimental metasomatic analogs. Plyusnina et al. (1995) performed several experiments with granite–dunite interactions in H_2O-chloride solutions at 400 and 500°C and 0.1 GPa to model ultramafic blackwall zones. At 500°C, a 2-mm zone developed between the contrasting rock types, in which the following subzones formed:

$$\begin{aligned}(\text{tonalite}) &- (\text{Ab} + \text{Na-amphibole} \pm \text{quartz}) \\ &- (\text{oligoclase} + \text{Tlc}) * (\text{Tlc} + \text{Di}) \\ &- (\text{Tlc} + \text{Ol}) - (\text{dunite})\end{aligned}$$

The asterisk marks the initial boundary.

At 400°C, the zoning was similar, but a chlorite zone appeared in place of the talc + diopside zone. Si appeared to be most mobile, becoming depleted in the marginal granite. Na was also mobile. Mg migration from the dunite was negligible, creating only some talc with plagioclase on the granitic side of the initial contact. Ca migration into the dunite resulted in the generation of diopside.

Vidale (1969) in the United States performed some experiments on juxtaposed calcite and model pelite, in saline (chloride) solutions, producing zoned skarns at the contact. The bulk of the experimental work on skarns, however, is also Russian (see Zharikov and Zaraisky, 1991; and Zaraisky, 1991, for reviews). Experimental charges are generally set up as an initial column in an open inert platinum capsule with powdered marble at the bottom and a powdered silicate rock at the open top. Capsules are surrounded by an aqueous (commonly alkali halide) solution that can enter the open end of a capsule and permeate through the silicate into the carbonate. Runs generally last two weeks. Results are usually a series of discrete zones through which the composition of the rock adapted consecutively and step-wise to the infiltrating fluids, approaching a state of local equilibrium across the column. Figure 31 shows an example of a traverse across a section cut through an experimental charge after two weeks at 600°C and 0.1 GPa (see also the back cover). Notice the similarity between the zoning developed in the charge and some natural examples listed in Table 2. Motion of Si, Ca, Fe, Mg, and, to a lesser extent, Al is required to produce the observed zoning.

It is possible to control and vary the rock types, fluids, and conditions in these experiments. Because the initial contact is also known, experimental results can be useful in constraining models of zone growth and development. Of course high temperature and the presence of a fluid phase are both conducive to chemical mobility, but the presence of a chloride brine appears to be equally important in facilitating metasomatism. When a 1.0 molar NaOH solution was used in the experiments, the granodiorite hydrated and albitized due to the Na content, but only a tiny and poorly developed contact zone of wollastonite formed (Zaraisky, 1991). The number of zones that form depends upon both the chemical complexity of the initial contact and the experimental conditions. The accumulated results of these and future experiments will greatly help constrain quantitative models of metasomatism.

The pioneering work of D.S. Korzhinskii has led to a fruitful approach to the study of metasomatic rocks, in the field, in the lab, and on the computer. In the words of Zaraisky (1993):

> Nearly all the principal propositions of Korzhinskii's theory of metasomatic zoning have been proven by experiment and computation. Most important of all is the strong numerical proof of the previously intuitively accepted assumption that the direction of metasomatic processes and the fundamental features of metasomatic zoning are controlled by thermodynamic relationships, and that the structure of any column, including those initially in a state far from equilibrium, in due course asymptotically approaches local equilibrium.

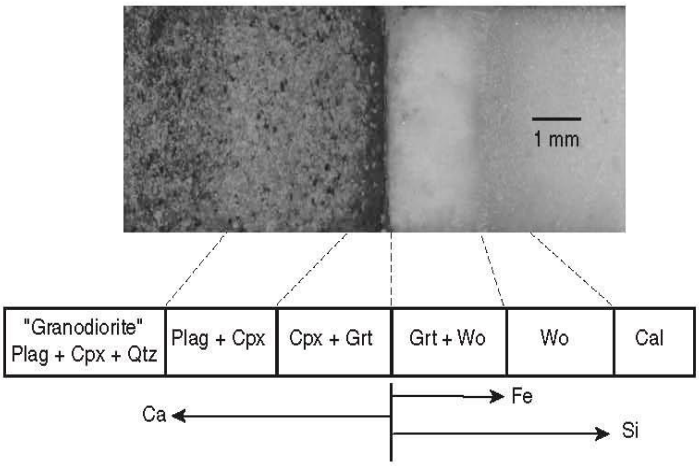

FIGURE 31 Zonation in an experimental skarn formed at the contact between granodiorite and limestone at 600°C, P_{fluid} = 0.1 GPa (X_{CO_2} = 0.07). After Zharikov and Zaraisky (1991). Photo courtesy G. Zaraisky.

Summary

Fluids play a critical role in many geologic processes. Fluids can dissolve material, transport heat and solutes, precipitate minerals, exchange components as they react with minerals, enhance partial melting, and catalyze deformation processes by weakening rocks. Deep fluids are typically supercritical mixtures dominated by C-O-H and typically richest in H_2O and CO_2 (and perhaps CH_4 at low temperatures and in more reducing conditions). Dissolved nonvolatile species tend to be dissociated into ions at lower temperature and higher pressure and more associated at higher grades. Most fluids are chloride brines with $NaCl > KCl > CaCl_2 \gg MgCl_2$. Aqueous SiO_2 is also typically present, as are bicarbonate, sulfate, and bromide.

In general usage, metasomatism is considered to involve the migration of appreciable nonvolatile material into or from a rock during metamorphism. Such migration involves mass transfer via either diffusion of matter through another medium (minerals or intergranular fluid) or as dissolved species carried along by infiltrating fluids (or both). Diffusion is *very* slow through minerals, but may approach a few meters per year through (intergranular) fluids. Estimates of time-integrated fluid fluxes suggest that huge quantities of fluid can pass through crystalline rocks ($\sim 10^3$ m^3 of fluid through each m^2 cross section of rock during regional metamorphism and perhaps 100 times that in channelized flow). Such flow is capable of redistributing heat and matter, thereby affecting the style of metamorphism and the rocks produced.

If migrating species are not in equilibrium with the new host rock, they react with the rock, exchanging components with the solid phases until local equilibrium is attained (or at least approached). As fluid moves, it carries solute species and continuously exchanges them with successive rock volumes that it encounters, generally producing different reactions at different zones along the flow.

Diffusion is driven by chemical potential (μ) gradients: any component will diffuse (if possible) from areas of high μ to areas of low μ. Diffusion (or infiltration) thus tends to reduce μ gradients. When effective, component mobility reduces the number of phases and generates discontinuities in X_{bulk}. The mineralogical phase rule may be expressed as $\phi \leq C_i$ where C_i is the number of "inert" (non-mobile) components. In cases of high mobility, C_i reduces to the lowest possible value (one) and monomineralic zones result. P-μ, T-μ, μ-μ, or log a-log a diagrams are useful in addressing systems with mobile components.

Reactions involving net transfer (i.e., migration) can be written in a number of ways, depending on what species are migrating. When matter is in motion it becomes difficult to determine original contacts between lithologic units, making the determination of a reference frame (what actually moved how far and in what quantity) a problem. Gresens-type and isocon diagrams are two attempts to solve the reference-frame and closure (sum to 100%) problems. We can successfully model some sequences of low-ϕ metasomatic zones that develop across initial contacts between rocks of contrasting composition using paths across μ-μ (or log a-log a) diagrams.

Key Terms

Supercritical fluid
Solubility product (K_{SP})
Dielectric constant
Dissociation constant (K)
Metasomatism
Diffusion
Bimetasomatism
Fick's law
Diffusion coefficient
Infiltration
Microfractures/hydraulic fracturing
Reaction-enhanced permeability
Flow-focusing
Thermal decompaction
Dilatancy pumping
Fluid:rock ratios
Time-integrated fluid flux (q_{TI})
Local equilibrium
Chemical potential
Mobile/immobile components
Activity
Isocon
Blackwall
Skarn/tactite
Endoskarn/exoskarn

Review Questions and Problems

Review Questions and Problems are located on the author's web page at the following address: **http://www.prenhall.com/winter**

Important "First Principle" Concepts

- Even dense crystalline rocks are capable of transmitting huge quantities of fluid during a period of regional metamorphism. Such flow can redistribute heat and dissolved constituents in both regional and contact metamorphism, profoundly affecting the style of metamorphism, as well as the composition and texture of metamorphic rocks.

- At equilibrium, the chemical potential of any component is the same in all coexisting phases. If gradients in μ exist, diffusion or infiltration will attempt to reduce the gradient (to zero, if migration is effective).
- A reduction in the number of coexisting phases and accompanying discontinuities in bulk composition (even where none existed before) are the hallmarks of metasomatic processes.

Suggested Further Readings

Metamorphic Fluids

Ague, J. J. (2003). Fluid flow in the deep crust. Chapter 3.06. *Treatise on Geochemistry*, **3**, 195–228. Elsevier. Amsterdam.

Bickle M. J., and D. McKenzie (1987). The transport of heat and matter by fluids during metamorphism. *Contrib. Mineral. Petrol.*, **95**, 384–392.

Bredehoft, J. D., and D. L. Norton (eds.). (1990). *The Role of Fluids in Crustal Processes*. National Academy of Sciences. Washington, DC.

Crawford, M. L., and L. S. Hollister. (1986). Metamorphic fluids: The evidence from fluid inclusions. In: *Fluid-Rock Interactions During Metamorphism* (eds. J. V. Walther and B. J. Wood). Springer-Verlag. New York. pp. 1–35.

Eugster, H. P., and L. Baumgartner. (1987). Mineral solubilities and speciation in supercritical metamorphic fluids. In: *Thermodynamic Modeling of Geological Materials: Minerals, Fluids, Melts* (eds. I. S. E. Carmichael and H. P. Eugster). *Reviews in Mineralogy*, **17**. Mineralogical Society of America. Washington, DC. pp. 367–403.

Ferry, J. M. (1994). A historical review of metamorphic fluid flow. *J. Geophys. Res.*, **99**, 15,487–15,498.

Ferry, J. M., and D. M. Burt. (1982). Characterization of metamorphic fluid composition through mineral equilibria. In: *Characterization of Metamorphism Through Mineral Equilibria* (ed. J. M. Ferry). *Reviews in Mineralogy*, **10**, Mineralogical Society of America. Washington, DC. pp. 207–262.

Ferry, J. M., and G. M. Dipple. (1991). Fluid flow, mineral reactions, and metasomatism. *Geology*, **19**, 211–214.

Fyfe, W. S., N. Price, and A. B. Thompson (1978). *Fluids in the Earth's Crust*. Elsevier. Amsterdam.

Labotka, T. C. (1991). Chemical and physical properties of fluids. In: *Contact Metamorphism* (ed. D. M. Kerrick). *Reviews in Mineralogy*, **26**, Mineralogical Society of America. Washington, DC. pp. 43–104.

Manning, C. E., and S. E. Ingebritsen. (1999). Permeability of the continental crust: implications of geothermal data and metamorphic systems. *Rev. Geophys.*, **37**, 127–150.

Schmulovich, K. I., B. W. D. Yardley, and G. C. Gonchar (eds.). (1995). *Fluids in the Crust: Equilibrium and Transport Properties*. Chapman & Hall. London.

Walther, J. V., and B. J. Wood (eds.). (1986). *Fluid–Rock Interactions During Metamorphism. Advances in Physical Geochemistry* **5**. Springer-Verlag. New York.

Metasomatism

Greenwood, H. J. (ed.). (1983). *Studies in Metamorphism and Metasomatism. Amer. J. Sci.*, Special Volume **283-A**.

Helgeson, H. C. (ed.). (1987). *Chemical Transport in Metasomatic Processes*. D. Reidel. Dordrecht, The Netherlands.

Hofmann, A. W., B. J. Giletti, H. S. Yoder, and R. A. Yund (eds.). (1974). *Geochemical Transport and Kinetics*. Publication **634**. Carnegie Institution. Washington, DC.

Korzhinskii, D. S. (1959). *Physicochemical Basis of the Analysis of the Paragenesis of Minerals*. Consultants Bureau. New York.

Korzhinskii, D. S. (1970). *Theory of Metasomatic Zoning*. Clarendon Press. Oxford, UK.